NASA Technical Memorandum 100771

A Review of Recent Research on Improvement of Physical Parameterizations in the GLA GCM

Y.C. Sud and G.K. Walker

December 1990

NASA Technical Memorandum 100771

A Review of Recent Research on Improvement of Physical Parameterizations in the GLA GCM

Y.C. Sud
Goddard Space Flight Center
Greenbelt, Maryland

G.K. Walker
Centel Federal Services Corporation,
Sigma Data Services Corporation
Greenbelt, Maryland

National Aeronautics and
Space Administration

Goddard Space Flight Center
Greenbelt, MD

1990

A Review of Recent Research on Improvement of Physical Parameterizations in the GLA GCM**

Y. C. Sud and G. K. Walker*

Global Modeling and Simulation Branch

Laboratory for Atmospheres, NASA/Goddard Space Flight Center,

Greenbelt MD 20771 (U. S. A)

ABSTRACT

A systematic assessment of the effect of a series of improvements in physical parameterizations of the the GLA GCM are summarized.

(a) The implementation of the Simple Biosphere Model (SiB) in the GCM is followed by a comparison of SiB-GCM simulations with that of the earlier slab soil hydrology GCM (SSH-GCM) simulations. The results demonstrate strong influence of vegetation on the surface energy balance, surface fluxes, and the hydrologic cycle. As compared to SSH-GCM, SiB-GCM produces less evaporation and more heating of the boundary layer over land which strengthens surface thermal lows (highs), with accompanying increase in moisture convergences (divergences) over land (ocean); this even affects the oceanic regions of 'roaring forties'. Excessive rainfall in Sahel, Northern Siberia, and North America is virtually eliminated in SiB-GCM simulations whereas strong thermally induced rainfall in the coastal regions of large continents continues to persist.

(b) In the Sahelian context, the biogeophysical component of desertification was analyzed for SiB-GCM simulations. Although, surface albedo and soil moisture anomalies have a positive feedback on the rainfall, the primary Saharan desertification process which supports northward march of Sahelian rain is surface evaporation. Reduced evaporation dries and warms the boundary-layer which leads

*Centel, Sigma Data Services Corporation, Building 22, NASA/GSFC, Greenbelt, MD..

**Paper presented at the Indo-US seminar on parameterization of subgrid scale processes in dynamic models of medium-range prediction and global climate. Aug. 6-10, 1990.

to dry convection instead of cumulus (moist) convection. Dry convection mixes the boundary-layer moisture into the sinking and diverging air aloft thereby providing an escape route to the PBL moisture that the strong solar heating helps bring into the region in summer (monsoon season). This mechanism has been verified in moisture transport calculations for model simulations and analysis of observations. Similar, though much weaker, influence of dry convection may be noted for the Thar Desert region of the Indian subcontinent.

(c) Cumulus parameterization is found to be the primary determinant of the organization of the simulated tropical rainfall of the GLA GCM using Arakawa-Schubert cumulus parameterization. An increase in the values of prescribed 'critical cloud work function' for different cloud types enables the GCM to produce time-mean cloud work function values that agree well with the Marshall-Island soundings used by Lord (1978). This modification has significant beneficial effects on the "spinup" problem. Two experiments invoking the limiting values of Arakawa-Schubert defined cumulus entrainment parameter, λ_{min}, helped us choose the Tokioka et al. (1988) suggested value for $\lambda_{min} = 0.0002\ m^{-1}$ for all cloud types.

(d) A comparison of model simulations with station data revealed excessive shortwave radiation accompanied by excessive drying and heating of the land. This leads to a very strong thermally induced inland convergence and coastal rainfall for large continents: North America, Africa and Asia. When mass-flux and relative humidity dependent fractional clouds together with climatological distribution of aerosols are used to allow cloud-aerosol-radiation interactions, the surface energy balance and the accompanying evapotranspiration become far more realistic giving a much better global rainfall climatology.

(e) The perpetual July simulations with and without interactive soil moisture shows that 30-40 day oscillations may be a natural mode of the simulated earth atmosphere system. It emerges with or without any changes in the time-mean external forcings: surface fluxes and solar declination. On the other hand, in a seven percent higher solar radiation case, which is consistent with the solar distance 9000 years ago, the results show a dominant 90 day time scale. This suggests that the time-scale of low-frequency oscillations represented by the first distinct EOF of a perpetual simulation can be modified by natural variations in solar forcing.

1. INTRODUCTION

A systematic evaluation of the influence of physical parameterizations in the Goddard Laboratory for Atmospheres (GLA) general circulation model (GCM) and some recent research to improve them are described in this paper. The version of the GLA GCM employed for this purpose has a resolution of 4^{o} latitude x 5^{o} longitude in the horizontal and has 9 sigma layers in the vertical. The model uses the primitive equations of motion to

solve for the future conditions of the atmosphere starting with given initial conditions of the atmosphere. The dynamical forcing is produced by parameterized physical processes. The prescribed daily varying sea surface temperatures (SSTs) and soil moisture are used to calculate prognostic surface fluxes.

This particular version of the model has been extensively used at the Goddard Laboratory for Atmospheres. Consequently, a comprehensive documentation of this model was produced by Kalnay et al. (1983, Vols I, II, and III). Until recently, the model was disseminated to the outside community as the official GLA GCM. The fourth-order finite differencing scheme for horizontal advection is due to Kalnay (see Kalnay et al., 1983, Vol. I, for a description of the numerical scheme) and the physical parameterizations: fluxes at the surface of the earth, dry and moist convection, cumulus and large-scale condensation, and short and longwave radiative flux divergences which include cloud radiation interaction, are either directly taken from, or are modified versions of the UCLA (University of California, Los Angeles) three-layer model (Arakawa, 1972). To adapt Arakawa's three types of cumulus clouds: shallow, mid-level and deep, (Arakawa et al., 1969), Sommerville et al. (1974) strapped the lowest six model layers into three 2 by 2 by 2 layers. Sud and Abeles (1980) modified the boundary-layer calculations to determine uniquely the near-surface air temperature and humidity, thereby eliminating the spurious 2-δt oscillations in surface fluxes; Wu (1980) developed the current longwave radiation (documented by V. Krishnamurthy, 1982) to replace the previous Hogan (1974) parameterization; and, Lacis and Hansen (1974) provided the state-of-the-art shortwave parameterization. Over the years, several other scientists have made various minor adjustments to the tunable physical parameters such as the drag and heat transfer coefficients over land and ocean to optimize model performance and to eliminate the systematic bias in the surface winds. Such modifications helped to obtain the best possible short range forecast with the model.

Within GLA, particularly in the Modeling and Simulation Branch, the model has been used for several weather and climate simulation studies (see for example, Baker et al.,1984; Atlas, 1987; Sud and Molod, 1988a and b; Wolfson et al., 1987), and satellite data impact investigations on weather forecast (Atlas et al., 1985; Halem et al., 1982; and Baker et al., 1984b). It has also been extensively used for 4-D data assimilation and satellite data retrieval work by Susskind et al. (1984, 1987), Atlas (1985) and Salstein et al. (1987).

To prepare the GCM for future global change studies which involve assessment of the behavior of the simulated atmospheric circulation and hydrological cycle in response to the slowly evolving earth-atmosphere system, we have made several improvements to the physical parameterizations of the model. We shall discuss the specific focus of our research by referring to the analysis of climate simulations with the model. The basic rule is that any systematic drift in the model's rainfall and circulation climatology warrants further investigations to determine the root cause for such behavior. The hope is that by a better understanding of the nature of model weaknesses, not only can improvements in physical parameterizations or numerical schemes be made but the role of processes producing the model deficiencies will also become self evident. In the majority of the case studies that we have pursued, this approach has pointed to weaknesses in physical parameterizations.

For the purpose of identifying areas requiring attention, we have relied heavily on the analysis of model integrations on the time scale of a month to a season; and, on that time scale, the influence of physical interactions largely dominate the outcome of the time-means as well as any systematic drift in the time evolution of circulation and rainfall. Our past work has been based on the following sensitivity studies on the roles of: i) surface albedo and soil moisture of desert border regions as given in Sud and Fennessy (1982 and 1984) and Sud and Smith (1985b); ii) evapotranspiration and dry convective processes in the Sahara Desert as given in Sud and Molod (1988a,b); and iii) a comparison of three different cumulus parameterizations (Geller et al, 1988). All these studies have led to the development of new parameterizations, some of which, in turn, have improved the simulations (i.e., effectively solved the problem being addressed) presumably for the right reason. In this pursuit, we have been successful in working out and implementing a few worthwhile modifications to physical parameterizations of the GLA GCM. A useful spin-off of this approach is that it reveals the underlying physical mechanisms that are responsible for maintaining as well as altering the global circulation.

An obvious limitation of a coarse resolution model such as this is that it is unable to resolve explicitly most of the important physical processes. These include boundary-layer fluxes, dry and moist convection, rainfall, fractional cloudiness with its dependent cloud-radiative forcing and turbulent eddy transport processes in the free atmosphere. Hence, the primary aim of any physical parameterization is to obtain the ensemble mean influence of the model's subgrid scale physical interactions from the grid scale prognostic variables (also called large-scale variables) so as to perform time integrations of the

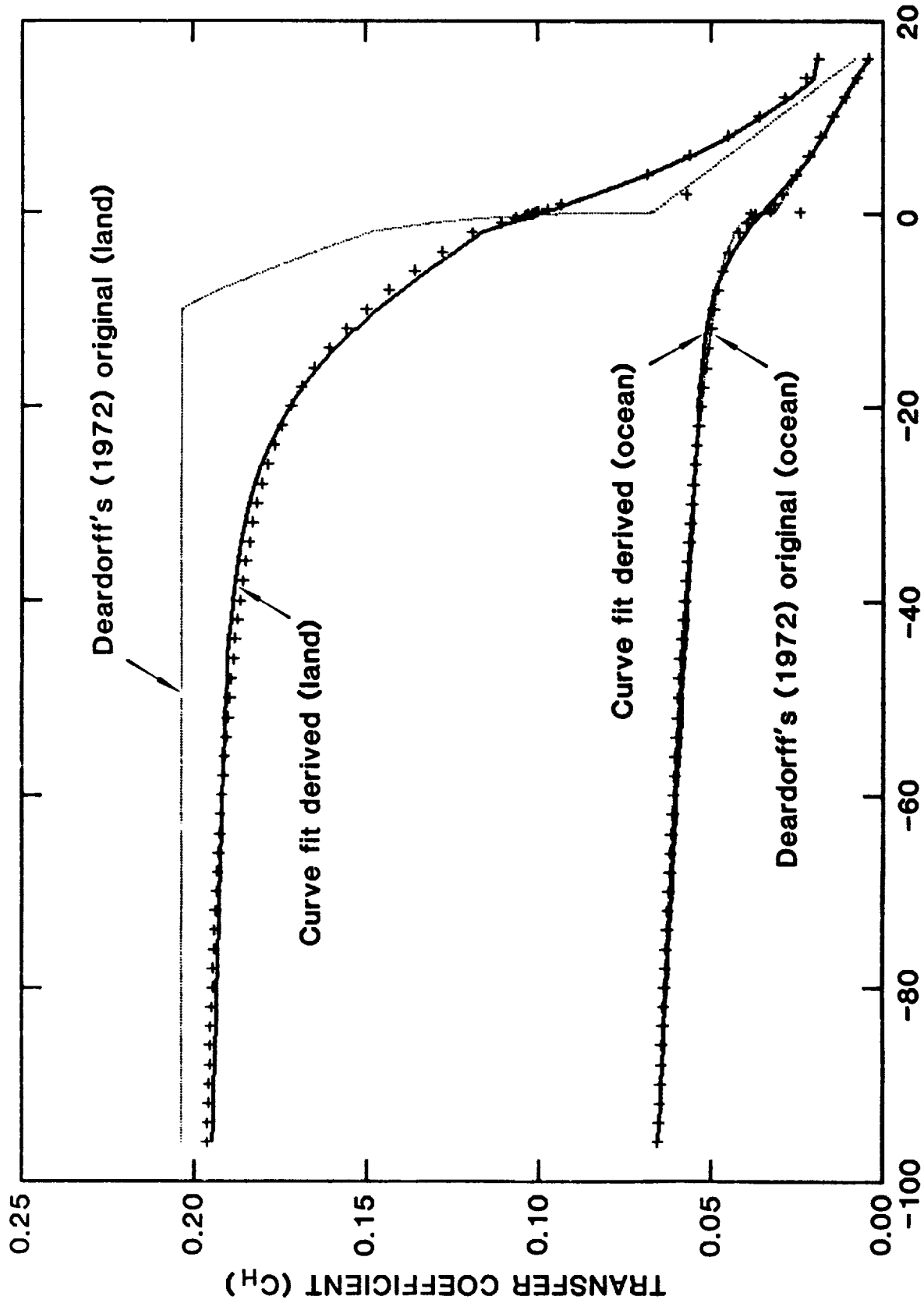

Figure 1. Bulk Drag (CD) and Heat Transfer (CH) coefficients for land and ocean as a function of Bulk Richardson's number. Deardorff (1972) formulae (dashed lines) and ensemble mean calculations (+ points) with curve-fit plots (thick solid line).

prognostic variable of the GCM. On the other hand, the coarse resolution model may be unable to resolve some important atmospheric wave activity: Kelvin and Rossby waves in the tropics, for example. To get them in the model, the only alternative is to increase the resolution.

It is important to recognize that the parameterization problem is fuzzy in nature. In other words, the very concept of subgrid scale parameterizability can be questioned. Actually, there is no proof that a physical system defined on a GCM grid-scale, with no subgrid scale constraints, is uniquely deterministic. In fact, simple considerations suggest that the subgrid scale variability is fully capable of giving a variety of end results for the same grid-mean conditions. For example, if a hypothetical boundary-layer air mass of the size of a GCM grid (about 400 km in the horizontal), were to advect over partly dry and partly wet land which evaporates heterogeneously, its subgrid scale humidity and temperature structure would be significantly different from that of the uniform subgrid scale temperature and humidity field distribution of another identical air mass that may advect over a homogeneously evaporating terrain while ingesting the same grid-averaged surface fluxes. It is easy to argue as well as to show to the unconvinced (using a very fine resolution model which resolves cloud processes) that the organization of subgrid scale convection that ensues in these two air masses would be vastly different. Since the subgrid scale variability under relatively quiescent (in the absence of strong mixing) conditions depends on the past history of the subgrid scale fluxes as well as the air mass modifications by the physical interactions, many possible subgrid-scale solutions for the same grid-averaged parameters could be expected naturally. How far these differences in subgrid scale parameters can affect the grid-averaged results is a question that has not been answered. To clarify what we mean by this, let us ask ourselves a fundamental question: is the physics of the averages essentially the same as the averages of the physics? The answer is YES, if the physical interactions can be assumed linear; nevertheless, the answer has to be NO, if the physical interactions are significantly non-linear. It is well known that the physical interactions are highly nonlinear; therefore, it is logical to hypothesize that subgrid scale variability strongly affects the spontaneous outcome of an ensemble mean grid-scale process; the only constraint being the limitations of the large-scale support and the scale selection for dynamical organizations in the atmosphere. Clearly therefore, the effect of subgrid scale variability on the physical interactions and future atmospheric evolution needs to be better addressed because one cannot directly apply concepts of homogeneous atmospheric interactions to grid-scale ensemble averages.

The above considerations allude to the non-unique character of the parameterizations of the subgrid scale processes, provided only grid mean values of prognostic physical variables are known. Recognizing the complexities as well as uncertainties involved in including the subgrid scale variability, the easiest alternative of ignoring all subgrid scale variability has been adopted by the atmospheric general circulation modelers in the past. Within those constraints, one can expect to do better by increasing model resolution so that unresolved subgrid structures get resolved and represented better. Alternatively, this situation can be improved by inferring subgrid scale variability in some ad-hoc manner and then assuming that it is randomly distributed. However, even that aspect of physical parameterization has not received much attention so far. *We believe that an ultimate solution to the problem of subgrid scale variability would require a grid-scale ensemble mean statistical mechanical model of the physical interactions.* However, such a model is not on the horizon, although there are indications that such work has already begun.

Sud and Smith (1984) show that the buoyancy dependence of bulk friction and heat transfer coefficients which are needed for the computing boundary-layer fluxes and which exhibit highly non-linear behavior about neutral buoyancy can be redefined to account for the subgrid scale variability. By simply assuming that the grid-mean field has a normally distributed subgrid scale variability and that its correlation with subgrid scale variability of other parameters involved in the earth-atmosphere interactions is negligible, Sud and Smith demonstrate that the bulk heat and momentum transfer coefficients: C_D, and C_H, as functions of Bulk Richardson number of the PBL (Planetary Boundary-layer) are much smoother as compared to the original Deardorff (1972) parameterized values for use in GCMs; whereas, the neutral buoyancy condition for the ensemble mean represent a stable PBL on the grid-mean variables (Fig. 1). These ensemble mean C_D and C_H functions were subsequently used in an earlier version of the GLAS GCM (described by Randall, 1982) and it was found that such a change can produce much more smoothly varying grid-mean estimates of surface fluxes. This zeroeth-order analysis shows a significant potential for better parameterization of the earth-atmosphere interaction. Presumably the same is true for many other physical interactions that exhibit non-linear behavior and large subgrid scale variability, such as cumulus convection, cloud-radiation interaction and boundary-layer turbulent transport processes. In fact it was possible to create an analytical relationship between C_D or C_H and the bulk Richardson number. This enabled us to calculate derivatives which, in turn,

helped to produce a stable scheme for the ground and surface air-temperature and humidity calculations with the slab soil hydrology (SSH) parameterization.

Another problem that may require attention in the near future relates to the resolved-versus-unresolved parts of a parameterization. In the current GLA GCM, for example, the cumulus clouds are resolved in the vertical but are unresolved in the horizontal (10-km cumulus scale vis-a-vis 400-km GCM grid scale). This situation demands vastly different considerations for the vertical and horizontal directions. Evidently, the existing cumulus schemes do address such issues; however, if a physical process is partly resolved and partly unresolved in any given direction, the problem of parameterization becomes far more complex. To the best of our knowledge, a systematic study of parameterizations for those situations has not been undertaken yet. An analysis of scale separation to isolate the fractional contribution from unresolved scales of the process, which may or may not be possible for a given physical process, must be conducted before any attempt can be made to parameterize the unresolved part. One can foresee that very soon modelers are going to be confronted with these kinds of problems, particularly with the increasing tendency for higher and higher resolution models which has become possible with the availability of super computers with mega-memories and gigaflop speeds.

In our experience, a majority of the systematic errors (drifts) in the simulations produced with the GLA GCM ultimately point to weaknesses in the physical parameterizations. This finding is corroborated by a) several shallow-water-type tests of numerical schemes which have shown remarkable reliability except for polar conditions; and, b) some dramatic reductions in the systematic errors of model simulations in response to improvements in the physical parameterizations in several case studies. The latter is also supported by some significant improvements in the climate simulations of the GLA GCM in response to several improvements in the physical parameterizations. Those are discussed in the next section.

In the context of the short-range weather prediction problem, another important question that must be addressed before starting to solve problem(s) related to data ingestion. Of the total root-mean-square (RMS) error of a short forecast on data insertion time-scales, which part is due to characteristics of error growth of the primitive equations, i.e., random errors of finite magnitude growing exponentially to produce a large error in future, and which part is due to deficiencies in the physical

parameterizations of the model? For example, let us consider the classic spinup problem in the context of the hydrologic cycle. The initial spike in the rainfall is related to two factors: inability of a cloud parameterization to ingest moisture fields without violently reacting to them, and the inability of the system to produce smoothly varying divergences. For the sake of discussion, we will direct our attention on the former situation. It is well known that in most of the models, the Arakawa-Schubert (1974) cumulus scheme rains out excessively after humidity field data ingestion in the tropics and after equilibration, creates conditions that are drier than the observed. On the other hand, the Kuo (1974) scheme, under identical conditions, is known to moisten the environment by shutting off rain during the equilibration process. Should one solve such a problem by improving the data assimilation scheme? The answer has to be NO, if the aim is to get to the root cause of the problem and work from there. However, in an operational environment, processes of nudging, such as proposed by Krishnamurti et al. (1984), and/or other solutions that effectively circumvent the problem, such as that proposed by Donner (1988, 1989) and Mintz (personal communication, 1987 suggesting elimination of water vapor assimilation until vapor distribution in the vertical produced by the model forecast, called the first guess, is closer to observations), are viable alternatives. We believe that data assimilation could be used as a vehicle to point out model weaknesses, but problems relating to the inability of a particular model to ingest observed data, without either rejecting or violently reacting to it, cannot be truly solved by improving the data assimilation schemes alone!

To determine whether a particular problem belongs in the model development or data analysis arena, diagnostic research is necessary. This can be followed by statistical analysis of attempts to simulate the well-known cases so as to identify the specific cause(s) of any given systematic error condition. The latter avenues have led to analysis (Cheng, 1989a,b,c) and parameterization (Cheng and Arakawa, 1990) of downdrafts, shallow convection (Tiedtke, 1984 and 1986), and evaporation of falling cumulus rain and vertical mixing of mass, heat, moisture and momentum during dry convection (Sud and Molod, 1988a). Thus, the data assimilation products serve to identify areas that require attention, but the improvement of data assimilation techniques cannot possibly solve problems emanating from model deficiencies.

Using the aforementioned methods of analyses while relying heavily on sensitivity studies of the recent past, we have identified several areas of weaknesses of the GLA GCM and have applied some ad-hoc corrections (tuning the free parameters, and/or introducing

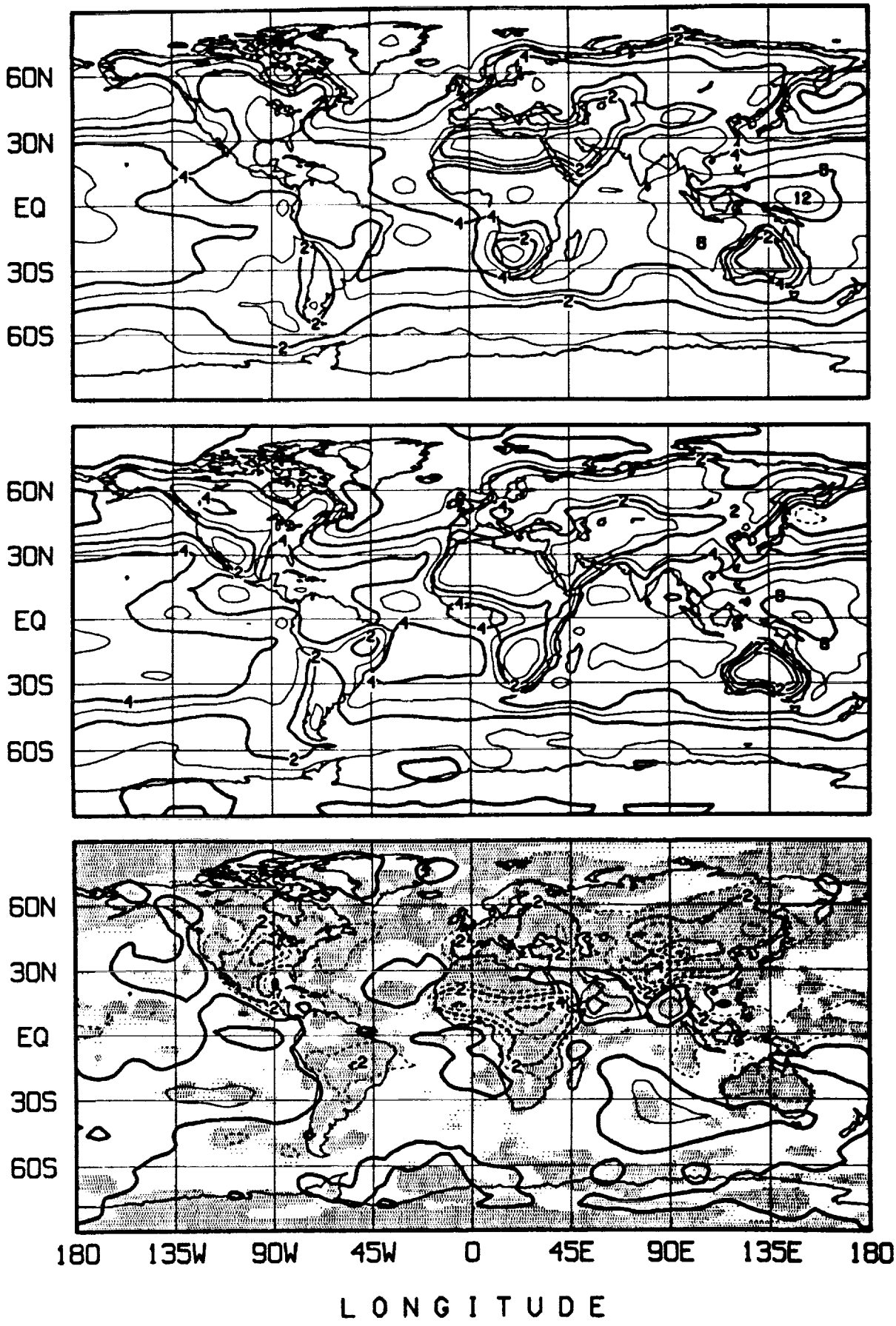

Figure 2a. Surface evaporation in mm/day for July simulations. *Top*: GLA GCM without SiB; *Middle*: GLA GCM with SiB; and *Bottom*: differences (SiB *minus* control) with shading for regions having better than 95% significance of mean differences when scaled with the pooled variability of the ensemble (contours for 1, 2 ,4, 6, 8, 10, 12 mm/day).

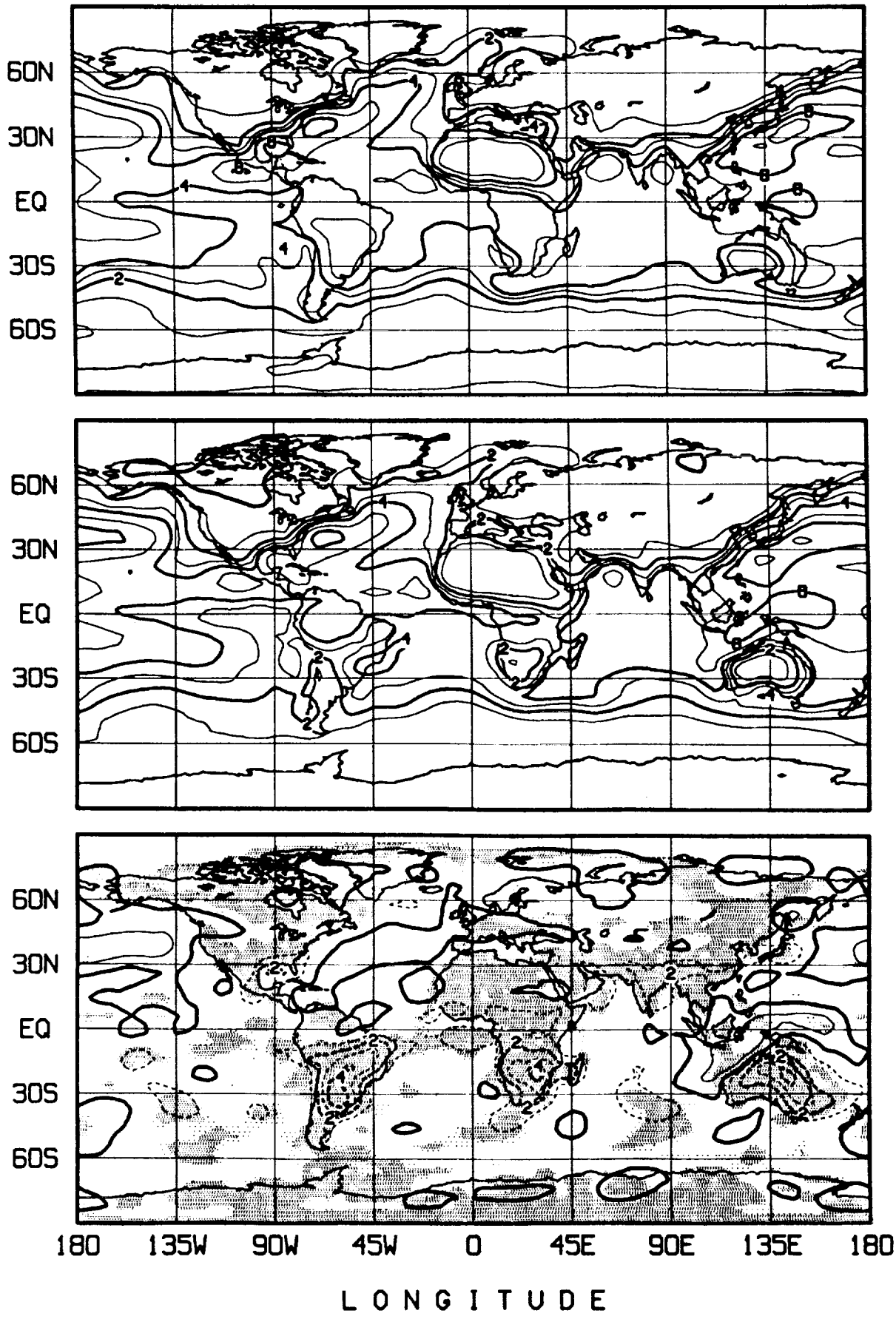

Figure 2b. Same as Fig. 2a, but for January simulations.

observationally based limits for containment of the inferred atmospheric interactions) as well as systematically developed new parameterizations for the GLA GCM. The successful results of such efforts are described below.

2. PHYSICAL PARAMETERIZATIONS

In this document, we shall address some of our work on physical parameterizations of the GLA GCM. To cover everything in a concise manner, we will not be able to reference fully other important works on the topic(s) under consideration; nevertheless, we have made every effort to include pioneering developments in the major areas of interest. The approach essentially relies on sensitivity experiments to isolate problems. We use diagnostics of model simulations for improvements and/or development of physical parameterizations to solve the problem under consideration. We also examine the internal consistency of assumptions and observational support for determining the reality of model produced atmospheric circulation, energetics, rainfall and atmospheric transports. Often, such analyses lead to the missing and/or weaker link(s) of parameterizations, thereby pinpointing areas requiring attention. Evidently, the above approach falls short of the ideals of developing a statistical mechanical model of physical interactions; however, in the recent past, the gains from even these types of improvements have been quite significant. We describe some results of systematic improvements in the physical parameterization of the GLA GCM and their influence on the model simulations under the following five subsections:

i) Land Surface Fluxes
ii) Ocean Surface Fluxes
iii) Dry and Moist Convection and Evaporation from Raindrops
iv) Land-atmosphere Interaction Simulations
v) Radiative Effects of Clouds and Aerosols

2.1 Land Surface Fluxes:

The research at GLA on the role of land surface processes goes back to the sensitivity studies with the GLAS GCM of the influence of land surface albedo of desert border regions (Sud and Fennessy, 1982). This work was a follow up on the pioneering surface albedo feedback hypothesis of Charney (1975) and his subsequent simulation experiments (Charney et al., 1977) with the GISS (Goddard Institute for Space Studies)

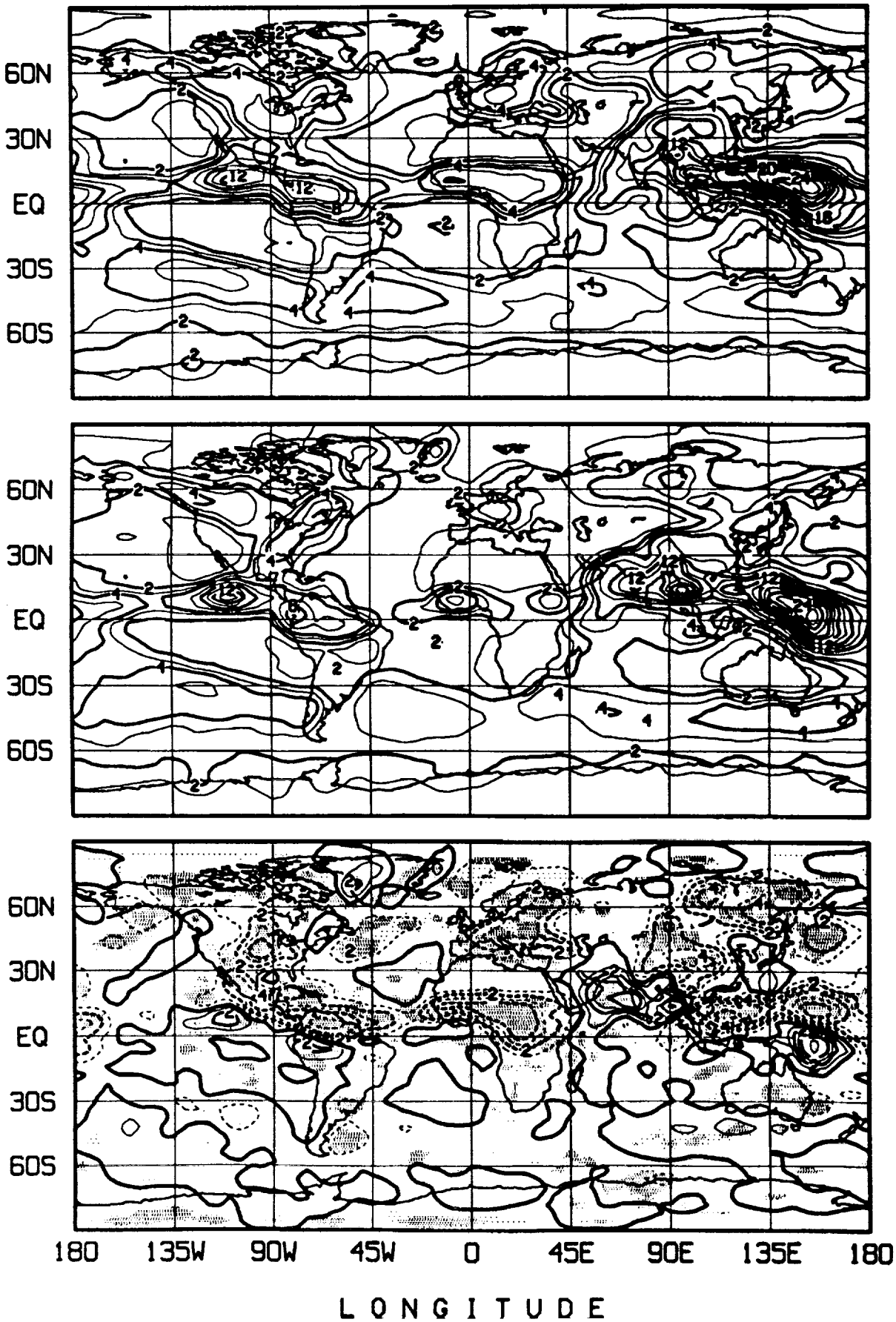

Figure 3a. Precipitation in mm/day for July simulations. *Top*: GLA GCM without SiB; *Middle*: GLA GCM with SiB; and *Bottom*: differences (SiB minus control) with shading for regions having better than 95% significance of mean differences when scaled with the pooled variability of the ensemble.

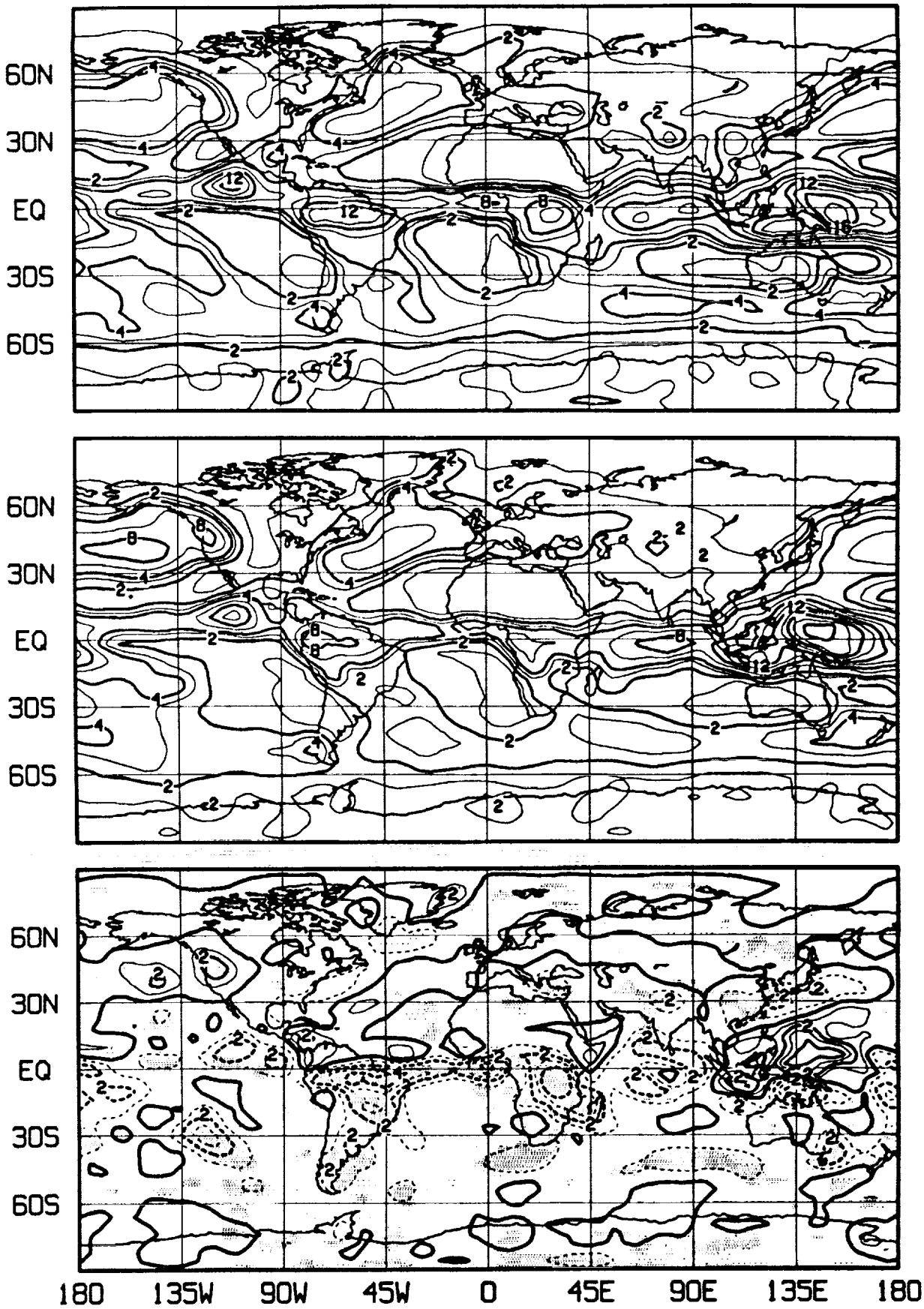

Figure 3b. Same as Fig. 3a, but for January simulations.

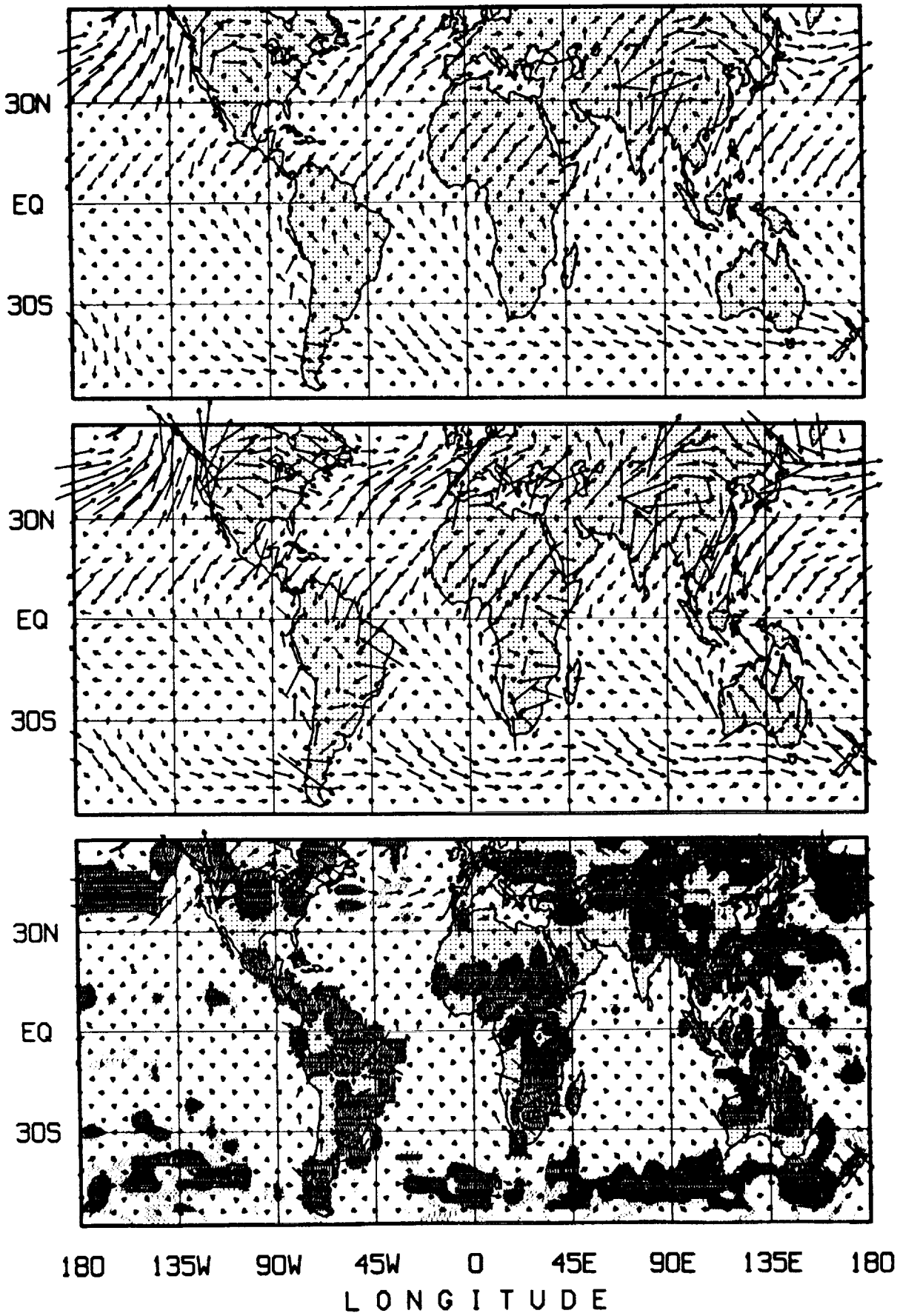

Figure 4. Surface-stress vectors for July simulations. *Top*: GLA GCM without SiB; *Middle*: GLA GCM with SiB; and *Bottom*: differences (SiB *minus* control) with shading for regions having better than 95% significance of mean differences when scaled with the pooled variability of the ensemble (5 degrees long. equals 0.1 N m^{-2}).

GCM, a predecessor of the current GLA GCM. The experiments were specifically aimed for determination of the role of bio-geophysical component of the desertification process. Subsequently, the soil moisture sensitivity study in the very same regions (Sud and Fennessy, 1984) was motivated by soil-moisture sensitivity work of Manabe (1969, and 1975) and Walker and Rowntree (1979). A recent study on the influence of the surface roughness of deserts (Sud and Smith, 1985a) was aimed at solving the problem of spurious rainfall in the Sahara in July simulations. This led to a suite of additional studies on the role of land surface roughness. One of these studies was for the Indian subcontinent (Sud and Smith, 1985b) and one was on the role of the surface roughness of all land (Sud et al., 1988). The latter study was designed following the method of an earlier well known work of Shukla and Mintz (1982) which shows, quite dramatically, the influence of land surface roughness on rainfall. Even though the winds increase over smoother land, the cross isobaric moisture transport convergence and rainfall into regions of semi-permanent lows reduces significantly. In this way, the study demonstrates the importance of parameterizing land surface roughness effects realistically. These studies together with several others (described in section iv) have not only clearly demonstrated several deficiencies of the simulated hydrologic cycle but also established the need for an improved parameterization of land surface fluxes.

The so-called bucket model of Budyko (1958) with variously tuned soil moisture availability function-β, as adapted by Manabe (1969) and Arakawa (1972) and several other major modeling groups throughout the world, was unable to give realistic evaporation over most land regions. For instance, on monthly averages, it gave excessive evaporation over sandy deserts. We now know that the slab soil hydrology model (SSH) is incapable of producing the biophysical controls of vegetation in response to ambient temperature, photosynthetically active radiation (PAR), rainfall interception and its re-evaporation from vegetation canopies. Thus, these studies along with several others: Walker and Rowntree (1979); Henderson-Sellers and Gornitz (1984); Laval (1983); Yeh et al. (1984); Laval and Picon (1986); Cunnington and Rowntree (1986); Xue et al. (1989), laid the foundation for the development of a physically realistic parameterization for the land surface fluxes. Consequently, a major effort was expanded to develop realistic vegetation parameterizations. Currently, there are several state-of-the-art vegetation models that are being used in GCMs; for example,SiB (Simple Biosphere model) of Sellers et al. (1986) and BATS (Biosphere Atmosphere Transfer Scheme) of Dickinson et al. (1986).

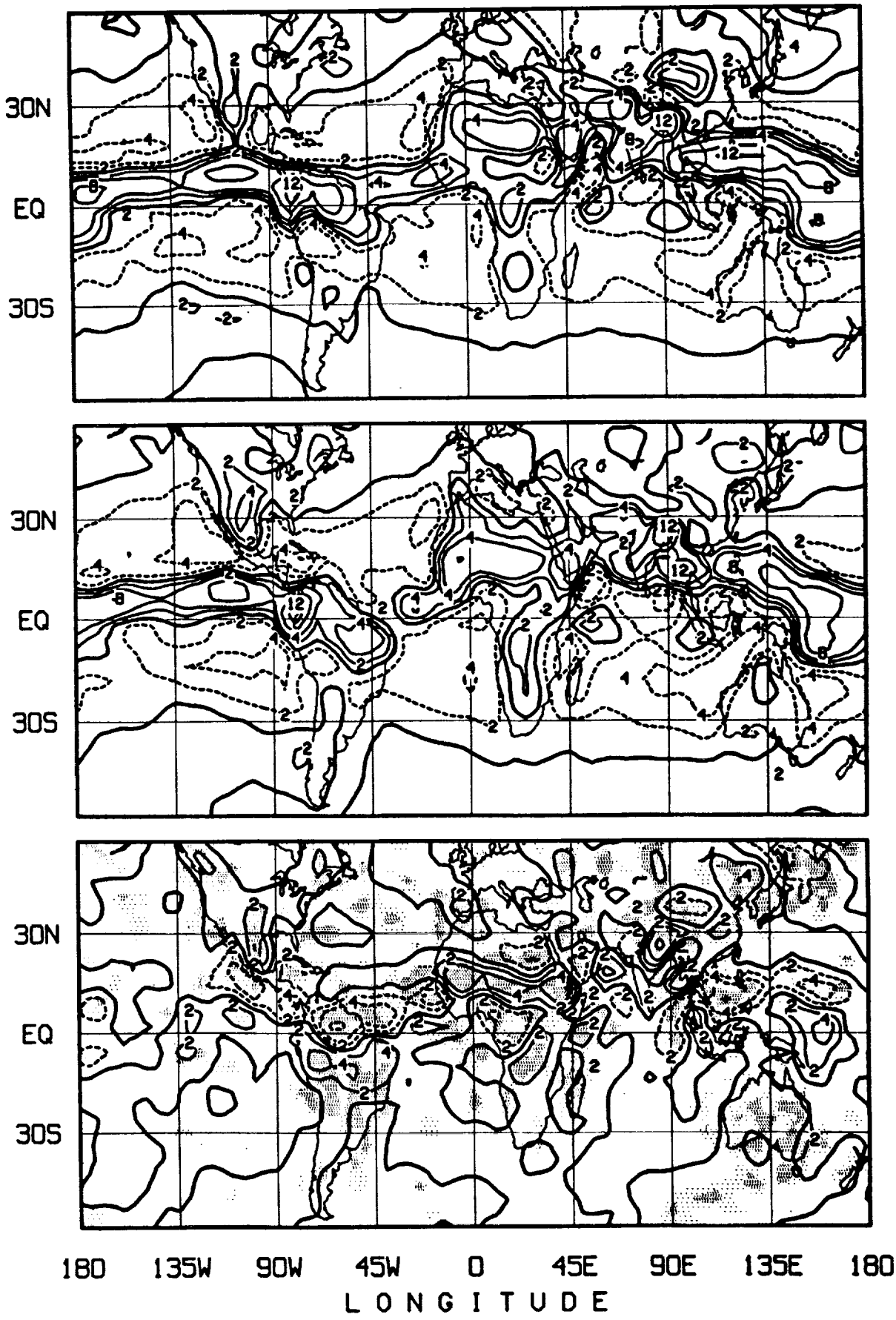

Figure 5. Moisture convergence in the PBL in mm/day for July simulations. *Top*: GLA GCM without SiB; *Middle*: GLA GCM with SiB; and *Bottom*: differences (SiB *minus* control) with shading for regions having better than 95% significance of mean differences when scaled with the pooled variability of the ensemble.

The Simple Biosphere model (SiB) of Sellers et al. (1986) was implemented in the Goddard Laboratory for Atmospheres (GLA) General Circulation Model (GCM). SiB calculates land surface fluxes of heat, moisture, and momentum, as well as near-surface fluxes of shortwave and longwave radiation with an explicit parameterization of the key interaction processes among atmosphere, vegetation, and soil processes. The influence of including SiB in the GLA GCM was evaluated by comparing the monthly simulations produced by the model with and without SiB. For the latter, a hypothetical slab (also referred to as bucket) of soil is used for calculating the land surface fluxes. In this evaluation, four summer and four winter simulations with the SiB-GCM were compared with the corresponding SSH-GCM. Several interesting differences are seen in these simulations.

In the following discussion, we shall mostly refer to July simulations and their differences with the two GCMs: SiB-GCM and SSH-GCM. Figures 2a and b show the influence of SiB on evapotranspiration (hereafter evaporation) field. Some very significant differences are evident in the monthly evaporation over land. With SiB, deserts evaporate much less; and, the evaporation over most other land regions is quite realistic. SiB's diurnal cycle has been examined and validated by Sato et al. (1989) and Sud et al. (1990) against observations and SSH-GCM simulations for different regions of the world. In the northern hemisphere, the regions of excessive evaporation and rainfall for July simulations found in the SSH-GCM have virtually disappeared in SiB-GCM simulations. Accompanying this change, there is a significant improvement in monthly rainfall climatology of the region (Fig. 3). Sud et al. (1990) have determined that excessive local evaporation in the SSH-GCM simulations was partly contributing to the excessive precipitation in the region. Overall, the simulated circulation and rainfall climatology of SiB-GCM is superior to that of any of the previous versions of the GLA or earlier GLAS GCMs, (Kalnay et al., 1983 and Shukla et al., 1981).

Even the momentum exchange between the earth and the atmosphere has improved with SiB. In particular, the surface stresses are larger over forests and smaller over bare land regions regardless of orography (Figs. 4). However, the momentum exchange coefficient, C_D, which depends on the buoyant stability of the boundary-layer, shows a significant increase over land in response to reduced evaporation and larger surface roughness. This change, in turn, is accompanied by higher temperatures and higher sensible heat and longwave fluxes at the surface. In the ensemble mean, the above implies that the PBL in the SiB-GCM is more unstable and is therefore able to exchange

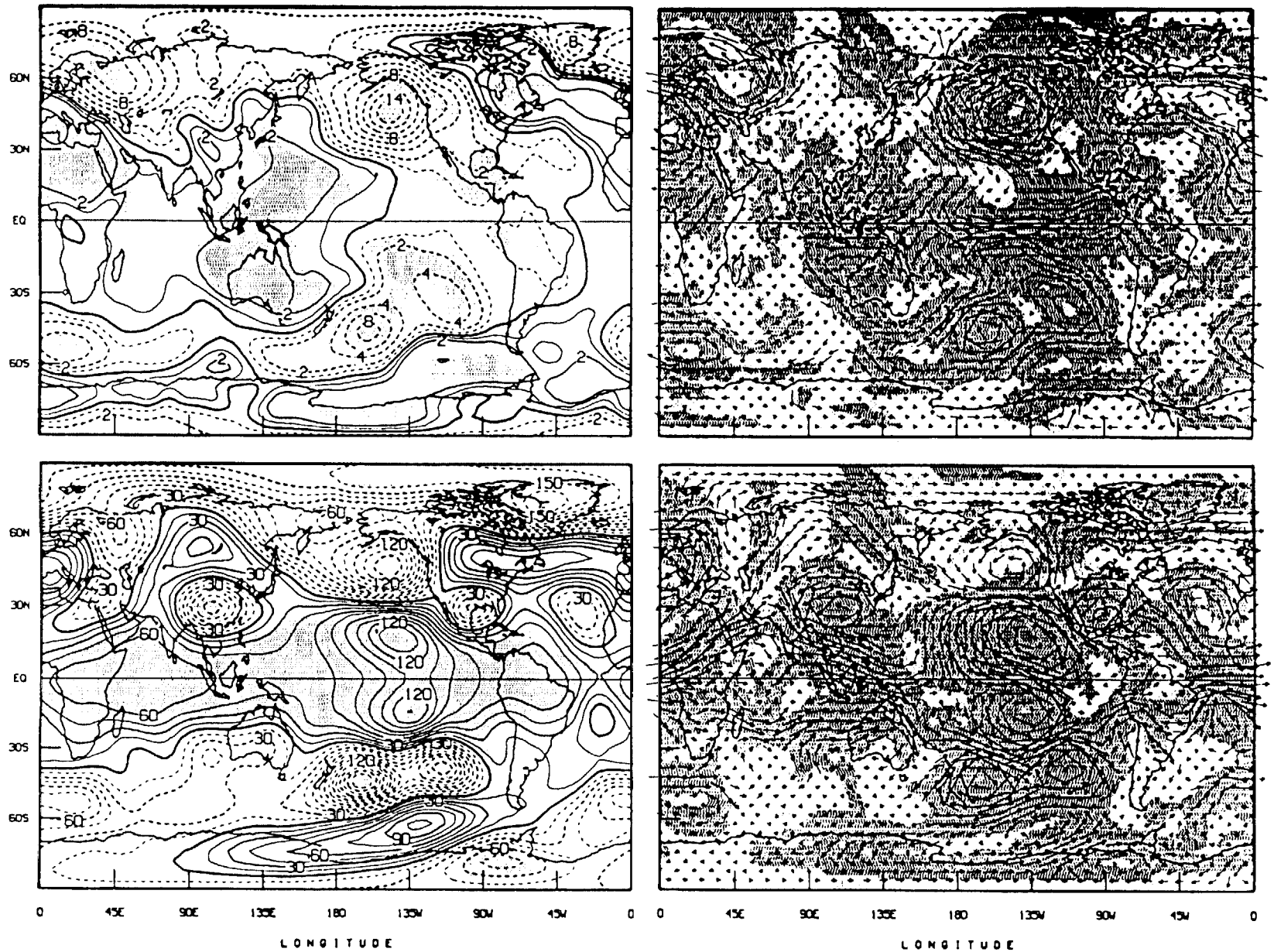

Figure 6a. Average January-February 1983 anomalies based on seven-year (1980-86) ECMWF analysis of obser-ions for *Top left*: sea-level pressure (mb); *Bottom left*: 200-mb geopotential heights in gpm; *Top right*: 200-mb winds (scale: 20 deg. longitude = 5 m/s *cos ϕ); and *Bottom right:* 850-mb winds (scale: 20 deg. longitude = 11.25 m/s *cos f). Shaded regions represent 90% (light) and 95% (dark) significant anomalies based on the student t-test for single or bivariate analysis.

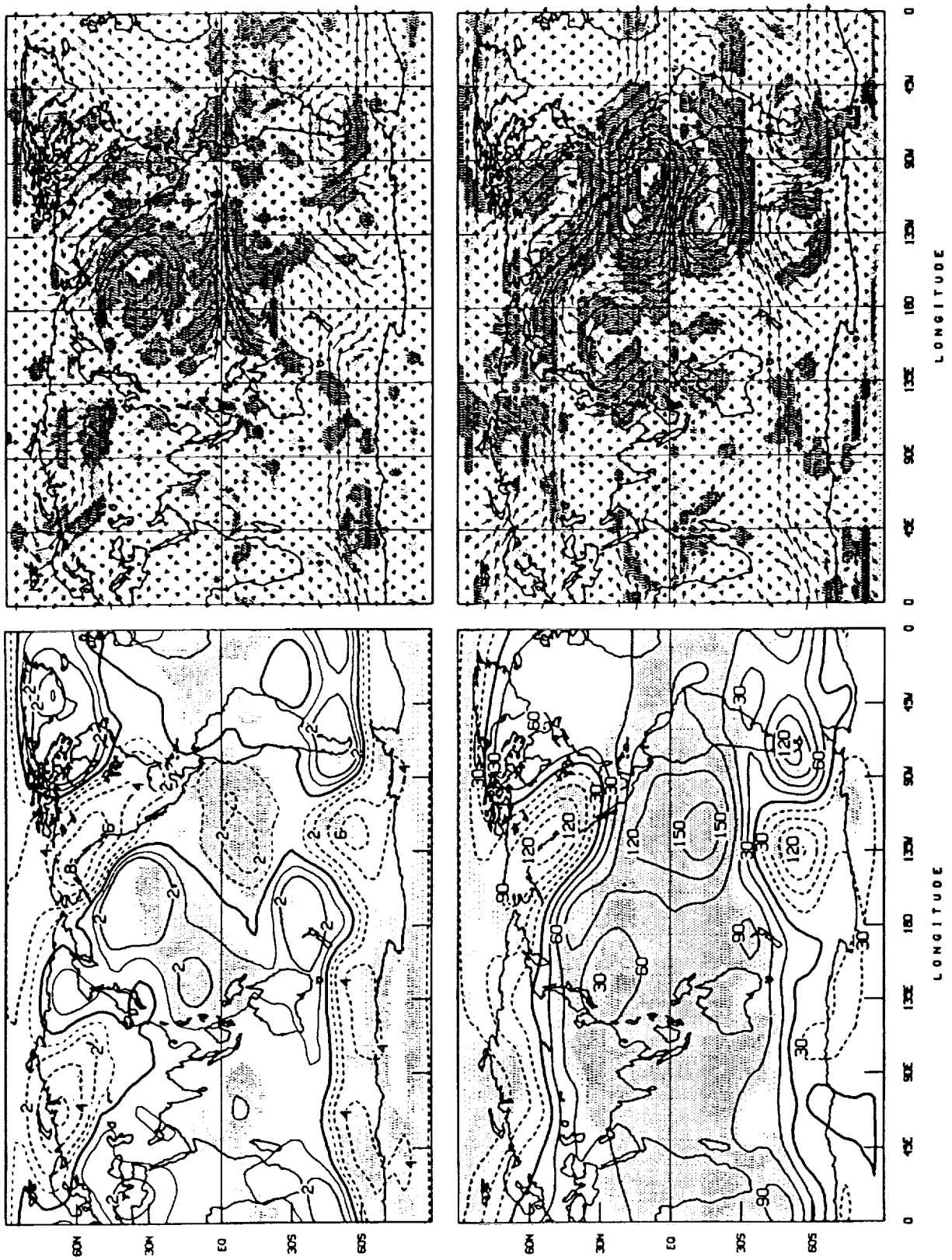

Figure 6b. Same as Fig. 6a, but for model simulations.

momentum much more efficiently with land. Consequently, SiB simulates weaker winds over land, particularly in the lower troposphere. Further details of this comparison can be found in Sud et al. (1990). SiB also produces changes in moisture convergence as a result of changes in the surface energy balance. The influence of SiB on boundary-layer moisture convergence for July simulations is shown in Fig. 5. It shows that SiB-GCM runs are associated with an increase in the moisture flux convergence inland, which accounts for the difference between the evaporation and precipitation. Since this moisture comes from the oceans, where the evaporation remains about the same, the precipitation over the oceans is correspondingly reduced in the SiB-GCM simulations. The picture is consistent with the SLP anomaly patterns that show a typical relative low over land and a high over the ocean, which is conducive to enhanced moisture flux convergence inland. SiB simulations also produce significantly larger boundary-layer moisture convergence in the Sahara Desert region. The moisture convergence is larger by 2-4 mm/day at the latitude of 15°N but the rainfall in SiB-GCM simulations is significantly less than that in the SSH-GCM simulations. The explanation is that with the reduced evaporation, but with about the same land surface heating by the sun, the dry convective mixing causes drying of the boundary-layer and moistening of the diverging airmass aloft. *This is the so-called water vapor mixing ratio dilution effect of the dry convective mixing of the PBL with the air aloft, which was pointed out by Sud and Molod (1988a) as the most important rain inhibiting process for North Africa, viz, the entire Sahara Desert as well as the Sahel region.*

2.2 Ocean Surface Fluxes:

Dependence of sea surface fluxes, particularly evaporation, on sea-surface temperatures is well recognized. The work at GLA on simulating circulation and rainfall for one El Niño: winter (January and February) 1983 and one La Niña year: summer (June and July) 1988, is reported in Sud et al., 1989 and 1990b, respectively. However, the sea surface fluxes also depend upon the ocean surface roughness and the near-surface wind speed, temperature, and specific humidity in response to atmospheric circulation; therefore, the net outcome of SST anomalies can be significantly swamped by systematic errors in the model's simulations. The primary motivation for the SST anomaly response simulations was to determine the ability of the GLA GCM to respond realistically to SST anomalies found during El Niño and La Niña episodes of the last decade. In the former case, we were generally successful in reproducing the tropical circulation: westerly wind anomalies over eastern equatorial Pacific at the 850 mb level and an

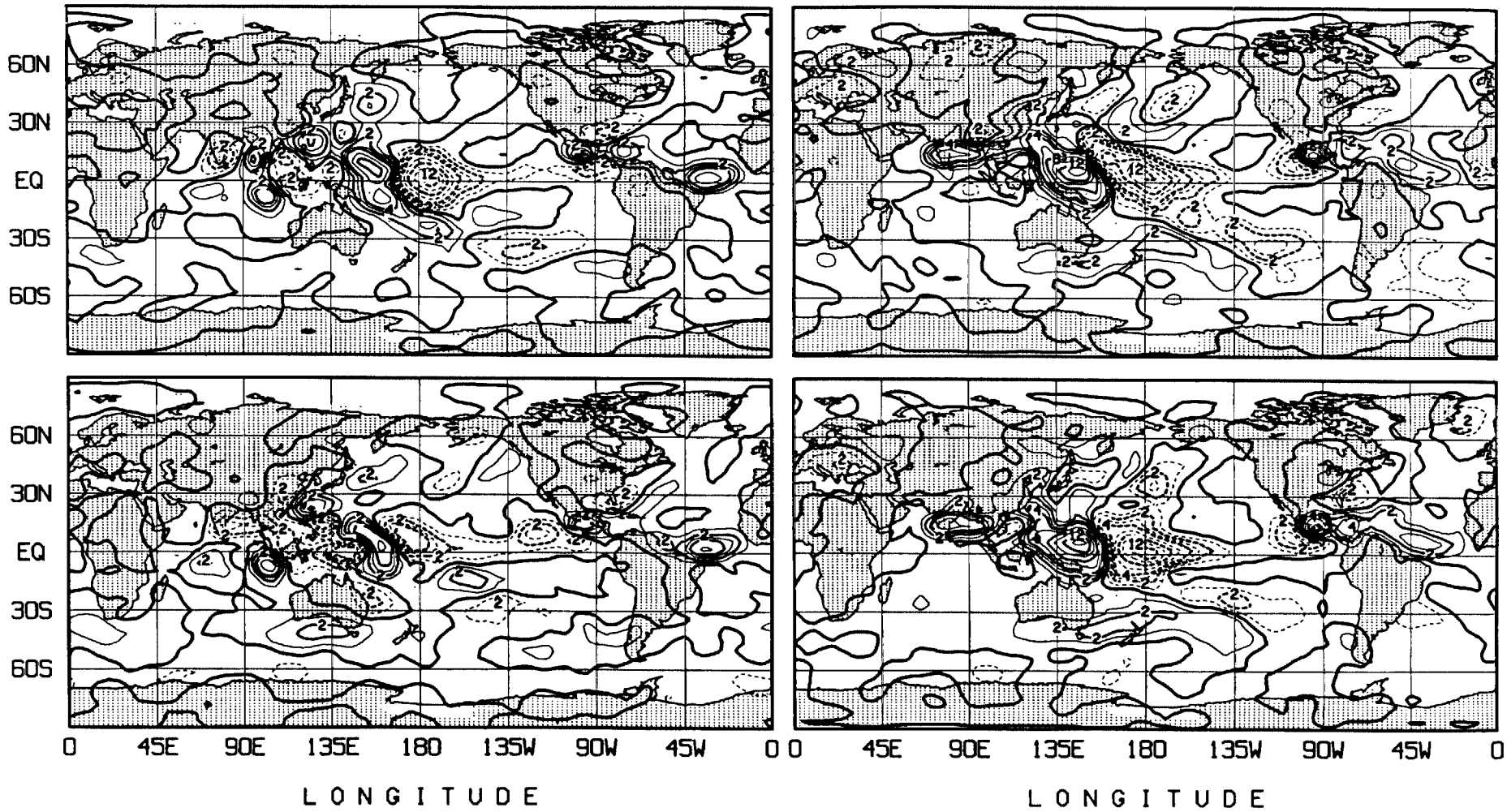

Figure 7a. Rainfall anomalies (mm/day) for June (left panels) and July (right panels) simulations for 1988. *Top*: SI minus I simulations; *Bottom*: SI minus C simulations. Contour intervals are 0, 1, 2, 3, 4, 6, 8, 10, 12, 14, and 16.

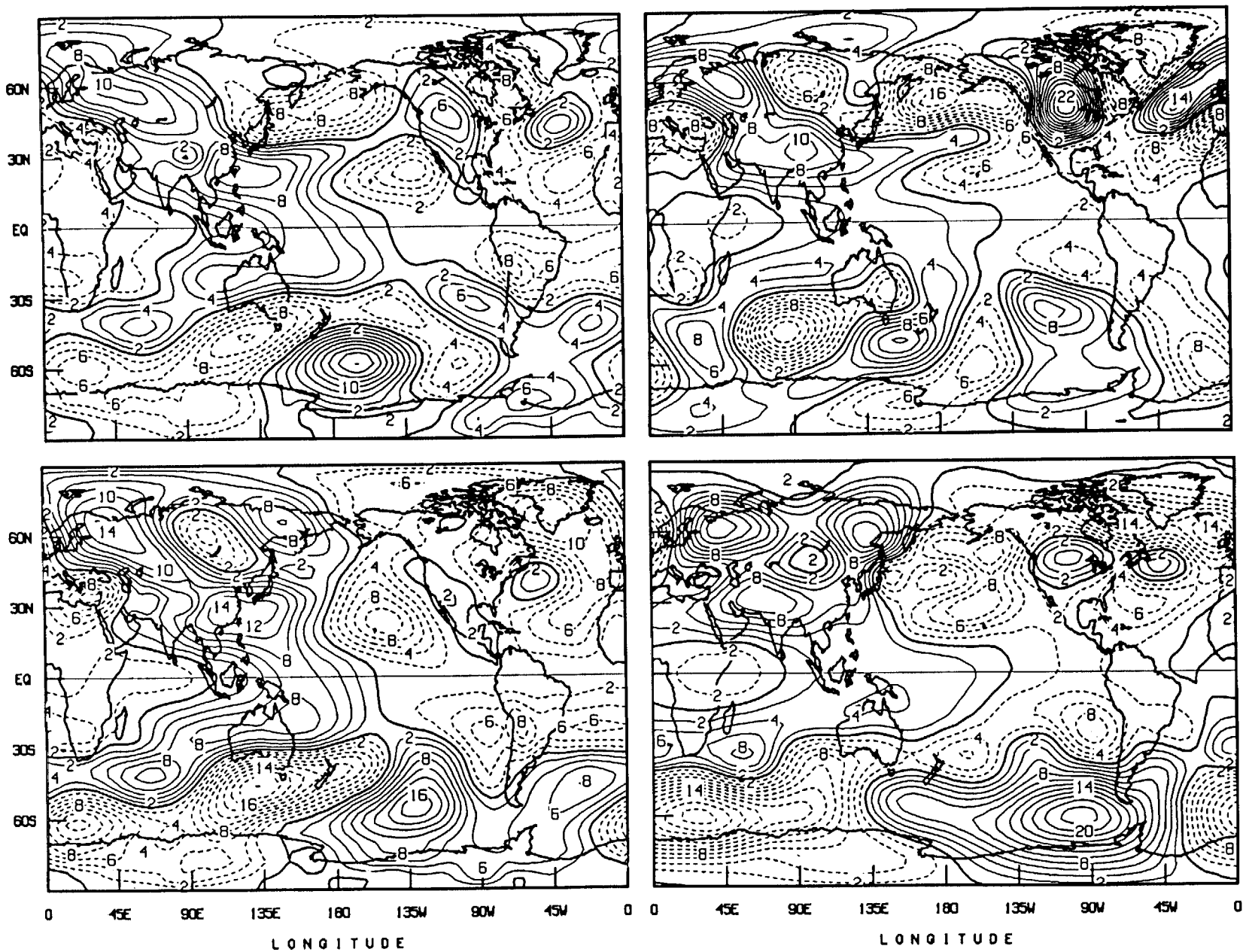

Figure 7b. The 200-mb geopotential height anomalies (dkm) as departures from zonal mean for June 1988 *(top)* and July 1988 *(bottom)*; model simulations (SI) are shown in the left panels and analysis of observations are shown in the right panels.

anticyclonic vortex couplet straddling the Equator at the 200 mb level. The rainfall anomaly features which contain increased positive rainfall anomalies between 120° W and 180° W over the equatorial eastern Pacific surrounded by a horseshoe-shaped region of reduced rainfall are also well simulated by the model. However, the model failed to produce a realistic mid-latitude response: see Figs. (6a, 6b) for comparison of model simulations with observations. Sud et al. (1988a) infer that this failure is the result of misplaced Rossby waves and the resultant stationary wave pattern. However, in contrast to this, Shukla and Fennessy (1988) who used the unimproved version of the earlier GLAS GCM have shown significant skill in the extratropics. Judging from this feature alone, one can infer that the model improvements may have degraded the model's ability to simulate climate anomalies but that is untrue as several monthly circulation and rainfall simulations suggest. We are currently looking further into this aspect of the model's weakness.

In a comparison of ensemble averages of simulated circulation between three control cases with climatological SSTs and three experiment cases with observed SSTs (obtained by superposing 1988 SST anomalies on climatological SSTs), Sud et al. (1990b) were able to simulate a weak, though realistic, rainfall anomaly representing drought conditions in June and the subsequent return of rainfall in July, 1988, Figure 7a. Moreover, the simulated circulation anomalies over North America also bear some resemblance with observations but the signal is much too weak, Figure 7b. We propose to include the soil moisture anomalies and expect that those, together with SST anomalies, will be able to produce a much more realistic simulation of the 1988 drought over North America. Namais hypothesized that the summer 1988 drought over North America was significantly affected by reduction in local evaporation (personal communications, 1989). That aspect of land-atmosphere interaction needs to be tested further. However, as the simulation experiments stand, we remain uncertain about the ability of GCMs to simulate the observed circulation features in the extratropics. For this case, some significant skill in 200 mb height anomaly predictions over North America was found by Mo et al. (1989) and Fennessy et al. (1990) in the NMC version of their GCM simulations.

2.3 Dry and Moist Convection and Evaporation from Raindrops:

Large sensitivity of simulated summer circulation and rainfall over North Africa to moist convection is established in all the July simulations with the GLA GCM. In the earlier versions of GLA/GLAS GCMs both Kalnay et al. (1983) and Shukla et al. (1981),

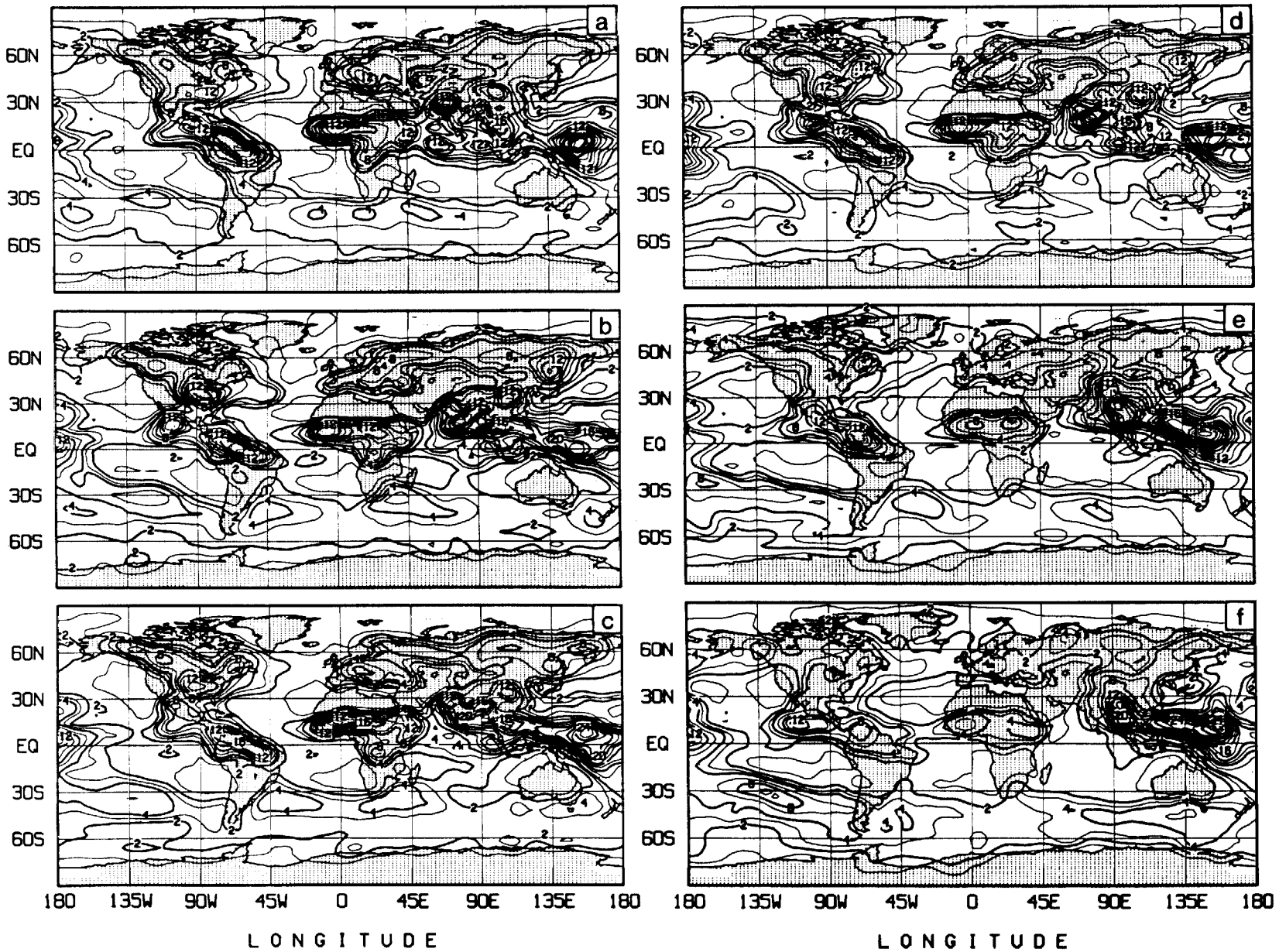

Figure 8. Total precipitation in mm/day. The arrangement of panels is as follows: a) Control with Arakawa-Schubert cumulus scheme; b) same as (a), but with moisture mixing in dry convection; c) same as (b), but with no relative 90% humidity restriction for the onset of moist convection; d) same as (b), but including momentum mixing in DCA; e) same as (d), but with Sud-Molod (1988) rain evaporation for all rain types; and f) same as (d), but with ad-hoc estimation for cumulus cloud-radiation interaction.

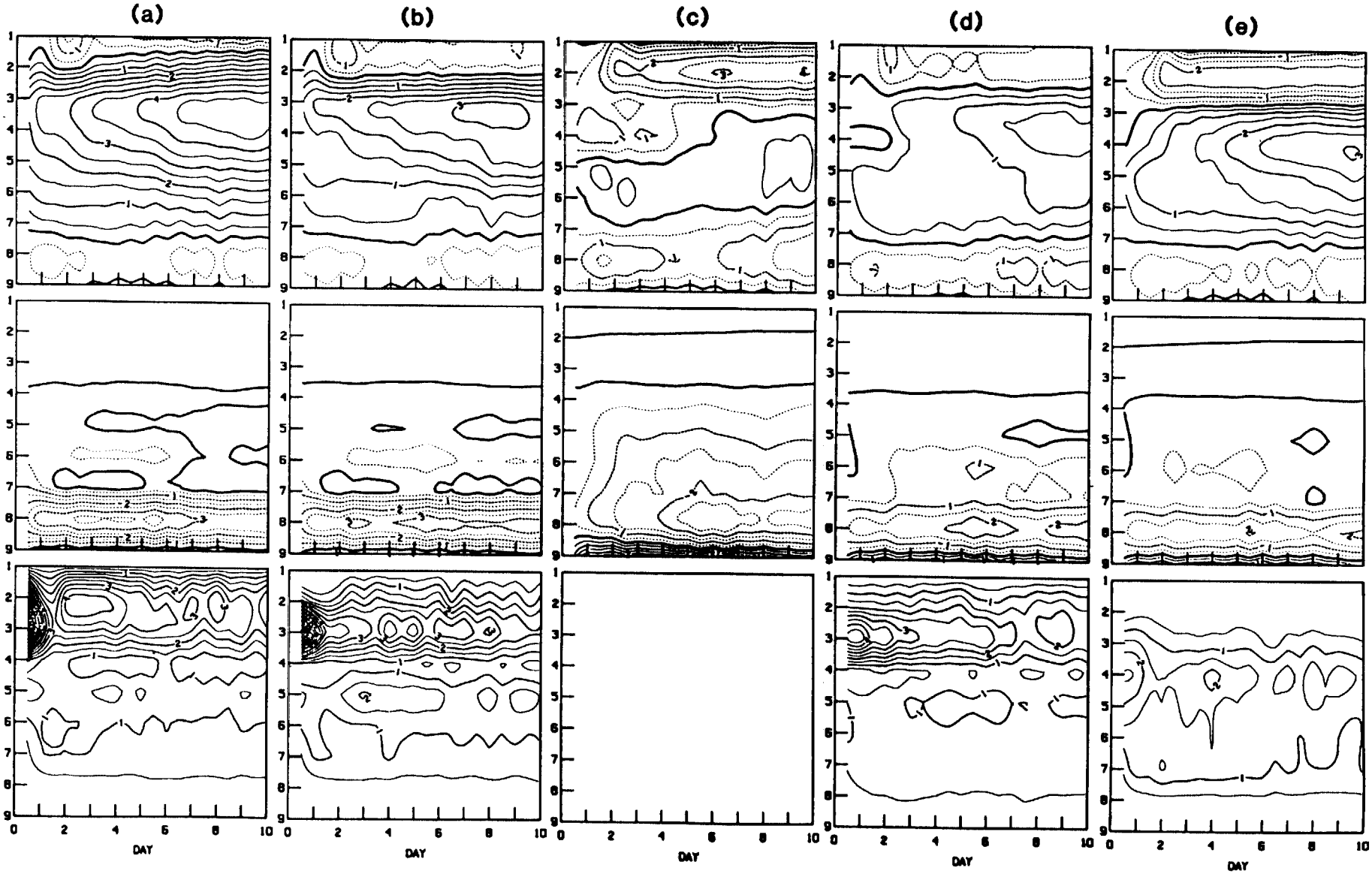

Figure 9a. Time series of Tropical (20N-20S) 12h mean fields of *Top*: precipitation in mm/day; *Middle:* Temperature difference simulated minus analyzed; and *Bottom*: specific humidity difference (simulated minus analyzed). Panel arrangement is a) Control; b) modified CCWF added to simulation (a); c) simulation (b) with cumulus convection disabled; d) λ_{min} limits determined from observed cloud radii added to simulation (b); and Tokioka et al. (1988) λ_{min} =0.0002. added to simulation (b).

This leaves only the top eight sigma layers to have convective clouds along with the associated latent heating and cloud-radiation interaction effects. However, both in nature and in the GLA GCM, the incidence of convective clouds in the top sigma layer, which typically represents the region of 10-120 mb thickness, is very rare. For a full understanding of the scheme the Arakawa-Schubert (1974) and other associated papers (Lord, 1978 and Lord et al., 1982) should be referred to.

Figure 8a shows that replacing the cumulus convection scheme of the model with the Arakawa-Schubert (1974) scheme did not significantly alleviate the problem of spurious rain in the Sahara Desert. However, in the process of computing airmass modification during dry convective adjustment, which for July conditions happens to be quite vigorous for the Sahara region, when the moisture was actually mixed along with mass and heat among the sigma layers involved in the adjustment, the rain in the Sahara disappeared, while producing a much stronger Inter-tropical Convergence Zone (ITCZ) that better resembles observations; Fig. 8b. This finding was followed by two more simulation experiments: one attempting to determine the roles of 90% relative humidity criterion and one designed to determine the sensitivity of the simulation to momentum mixing as shown in Figures 8c and d. Removal of the former constraint had very little influence on the monthly simulations, whereas invoking the latter produced several beneficial effects. The dry convective mixing for the last case is equivalent to total instantaneous mixing which, evidently, would be the end result of an eddy mixing process over a finite period of time. Consequently, the GLA GCM's dry convective parameterizations were modified to perform mixing of heat, water vapor, mass and momentum instantaneously among the layers involved. Indeed, the aforementioned dry convective mixing calculation produced a much drier Sahara in the model simulations. The actual mechanism worked in a very simple way. The boundary-layer moisture flux convergence into the local thermal low of the Saharan region was mixed by dry convection into the sinking and diverging air aloft thereby providing an escape route to the incoming moisture. This also explains why without the dry convective mixing of moisture, the simulated rainfall actually increases over the Sahara Desert even when the evaporation was reduced. It happens because the dry Sahara produced an even stronger thermal low with equally stronger moisture convergence into the boundary-layer, which, when disallowed to escape by mixing with the diverging air aloft had the only other option of escaping via cumulus convection which makes rain. Recently, the problem of spurious rain over the Sahara Desert has also been solved in most other GCMs, which also produced large amounts of spurious rain over the Sahara region in the past. This has been achieved

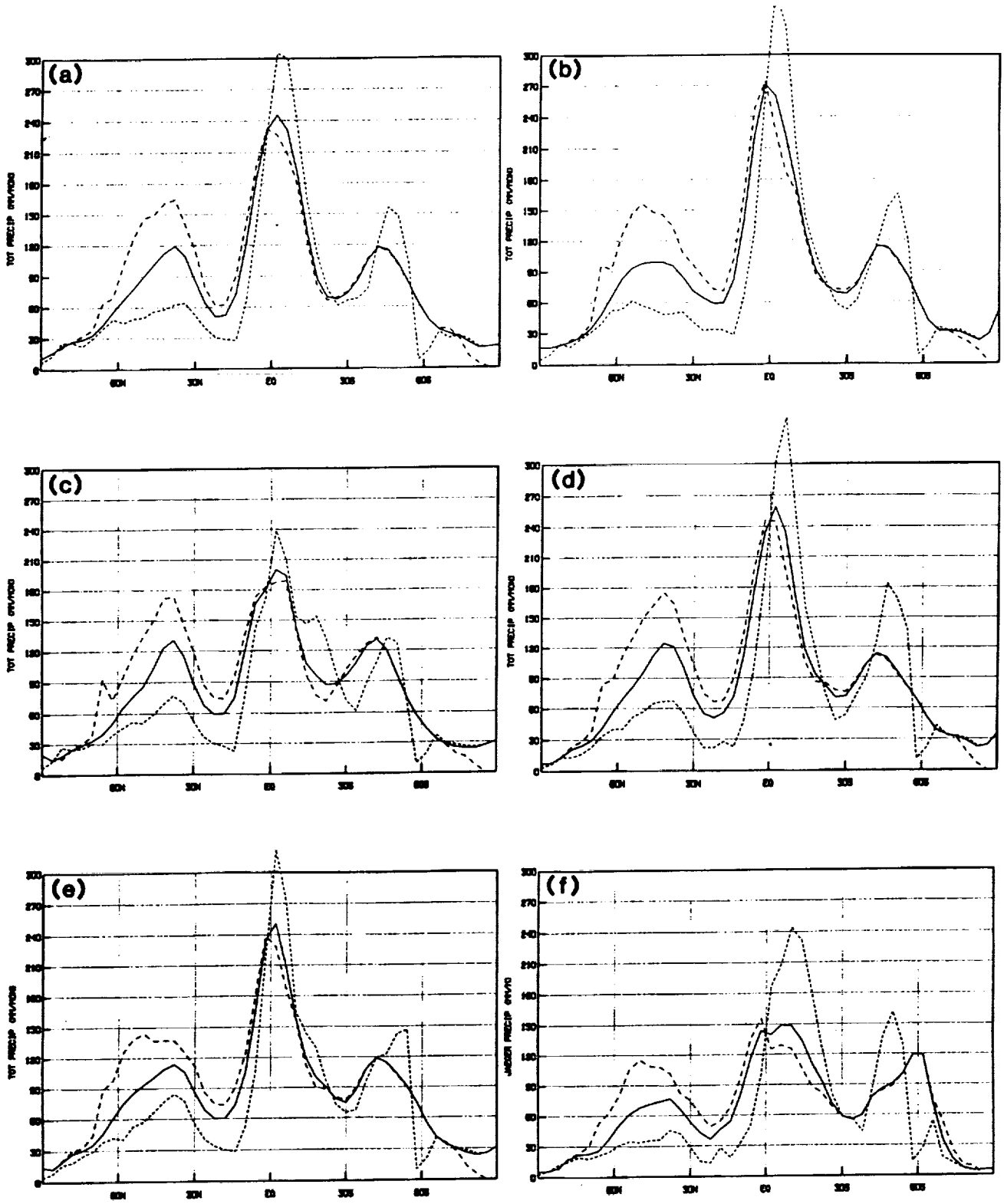

Figure 9b. Monthly fields zonal mean January precipitation in mm/day. Panel arrangement is a) Control; b) Modified CCWF added to simulation (a); c) simulation (b) with cumulus convection disabled; d) λ_{min} limits determined from observed cloud radii added to simulation (b); e) Tokioka et al. (1988) λ_{min} =0.0002 added to simulation (b); and f) Jaeger (1976) rainfall climatology.

as a consequence of introduction of shallow convection, turbulent entrainment and transports within a growing boundary-layer and inclusion of an assortment of eddy mixing calculations invoking different time scales. We claim that the key effect of all these different parameterizations for the Sahara region is to mix the moisture into the diverging air aloft which we have achieved by simple dry convective mixing that transports heat, moisture, as well as momentum aloft.

Figure 8e shows the influence of evaporation of falling rain on the rainfall in the Sahel and the Sahara regions. The current rain-evaporation parameterization (Sud-Molod, 1988) uses a physically based formulation to evaporate from falling raindrops. It takes into consideration the rainfall intensity, raindrop size distribution, humidity gradients, and sphericity influence of hydrometeors traversing the ambient air. In the global mean, the parameterization is able to evaporate about 43% of the falling rain whereas the documented value is roughly 40%. Thus, the parameterization is producing a realistic overall effect. For details of this parameterization, reference to Sud and Molod (1988, Appendix A) will be helpful.

Figure 8f shows the sensitivity of rainfall to convective cloud radiation interaction. Its influence is so strong that it led us to develop a parameterization for fractional clouds. This enabled longwave and shortwave cloud-radiation interactions which, in turn, have led to more realistic radiative heating of the atmosphere as well as the surface energy balance. We describe the parameterization in subsection v. With reference to the Indian subcontinent, the arguments made earlier for the Sahara region also apply. Briefly, these are as follows. Figures 8a and 8b show that there is excessive rain in the semiarid region of northwestern India where dry convection is significant whereas, Figs. 8e and f reveal a strong influence of inclusion of evaporation of falling rain and cumulus cloud-radiation interaction on the July rainfall climatology over the Indian subcontinent. Some other noteworthy features of this comparison are: a) significant improvement in the ITCZ formation and b) a large change in the Central American rainfall in response to inclusion of cloud radiation interaction, which reduces solar heating of large continents (North and South America) producing weakening of the monsoon-like circulation into coastal regions.

In order to alleviate the spinup problem (excessive rain and significant drying out at the initial time) as well to understand the role cumulus convection, three different experiments were conducted with the GLA GCM by Sud et al. (1989).

First, the effect of the prescribed critical cloud work function (CCWF) values that were derived and defined in a specific way by Lord et al. (1982) in the Arakawa-Schubert cumulus scheme was examined. It was evident that the CCWF values for different cloud types were contrived from the observed temperature and humidity profiles over the Marshall Islands (Reed and Recker, 1971). In reality, the Marshall Island data represents the time averaged cloud work function (CWF) for the observation period. Even if one can justify the general assumption that the entire tropical atmosphere maintains the typical Marshall Island time averaged CWF distribution, the second assumption that CWF equals CCWF can be easily improved. We have subsequently redefined the CCWF distributions for various cloud types such that they will yield the observed CWF distribution. Without going into the details of the process of determining the new CCWF value which are discussed in detail in Sud et al. (1989), we summarize the key results of these studies.

The CCWF perturbation experiments, in which CCWF was doubled for every cloud type, showed that the choice of CCWF has significant effect on the spinup problem. The relative vertical distribution of CCWF controls the onset of different cloud types. We have determined that increasing the threshold values of CCWFs for all clouds tend to concentrate the rainfall into a narrower ITCZ. They also affect the rainfall during the initial adjustment period. Moreover, the CCWF values were found to be a major determinant of the apportionment of convective and large-scale rain. Increasing (decreasing) the CCWF reduces (increases) the convective rain while increasing (decreasing) the large-scale rain but not necessarily in the same region. This result is easy to comprehend if one considers that as long as evaporation at the surface is not changed the water vapor added to the atmosphere has to come down as precipitation, and, if convective precipitation is diminished, the large-scale precipitation would increase to restore the balance between evaporation and rainfall.

Second, a monthly simulation without any cumulus convection was conducted to assess the role of cumulus convection. The results of this experiment were very surprising. Absence of cumulus convection did not appreciably lower the level of condensation heating or the magnitude of rainfall. This was indeed not the case in any of our previous model simulations with the original GLA GCM physics. We claim that it has happened in the current GLA GCM with all of the improvements (modifications described above) because near the surface the dry convective mixing or large-scale lifting helps to

transport the water vapor upwards where it condenses as large-scale rain. The resulting condensation heating sets up the temperature profile to promote dry convection into the next higher level. Thus, instead of moist convection helping to transport the moisture to the level of neutral buoyancy and produce the entire condensation heating in one step, disablement of moist convection produced heating by large-scale condensation and upward transport of moisture and heat by dry convection in a series of sequential steps each of which works on a half-hour time scale. This suggests that the large-scale condensation heating with dry convective mixing can be roughly equivalent to the resolved ensemble mean grid scale influence of moist convection. This would be precisely the case if moist convection was occurring on the resolved grid scale of the GCM. The results of the first 10 days of integration with the model are shown in Fig. 9a, whereas the zonal mean rainfall simulations are shown in figure 9b.

Third, the pioneering research of Tokioka et al. (1988) has shown how stipulating a minimum value for the entrainment parameter, λ_{min}, in the Arakawa-Schubert parameterization can affect the 30-60 day oscillation of a GCM simulation. Sud et al. (1990) experimented with the containment of the cumulus entrainment rate by invoking upper and lower limits on the entrainment parameter λ. Observations of radii limitations of different cloud types permitted us to put some realistic approximate limits on λ. The contrived distribution of λ bounds as a function of cloud type was obtained following Simpson's (1971) formulae. This simulation was compared with another simulation in which we used the Tokioka et al. (1988) recommendation for λ_{min} =0.0002. With the help of these experiments, we have established that the λ distribution also affects the anomalous rainfall simulation during spinup. An analysis of results of two sets of experiments described above have provided an effective solution for the spinup problem. This solution has a marked influence on the simulated relative humidity and temperature in the tropics. Much more data are required to provide the Arakawa-Schubert parameterization with observationally derived limits on λ-distributions. In the meantime, using a lower limit on the entrainment parameter following Tokioka et al. (1989) is retained. This correction has shown considerable promise in the Meteorological Research Institute (MRI) GCM in Japan. It may be pointed out that the overall performance of the Arakawa-Schubert cumulus parameterization in the GLA GCM in response to the changes described above has also improved significantly.

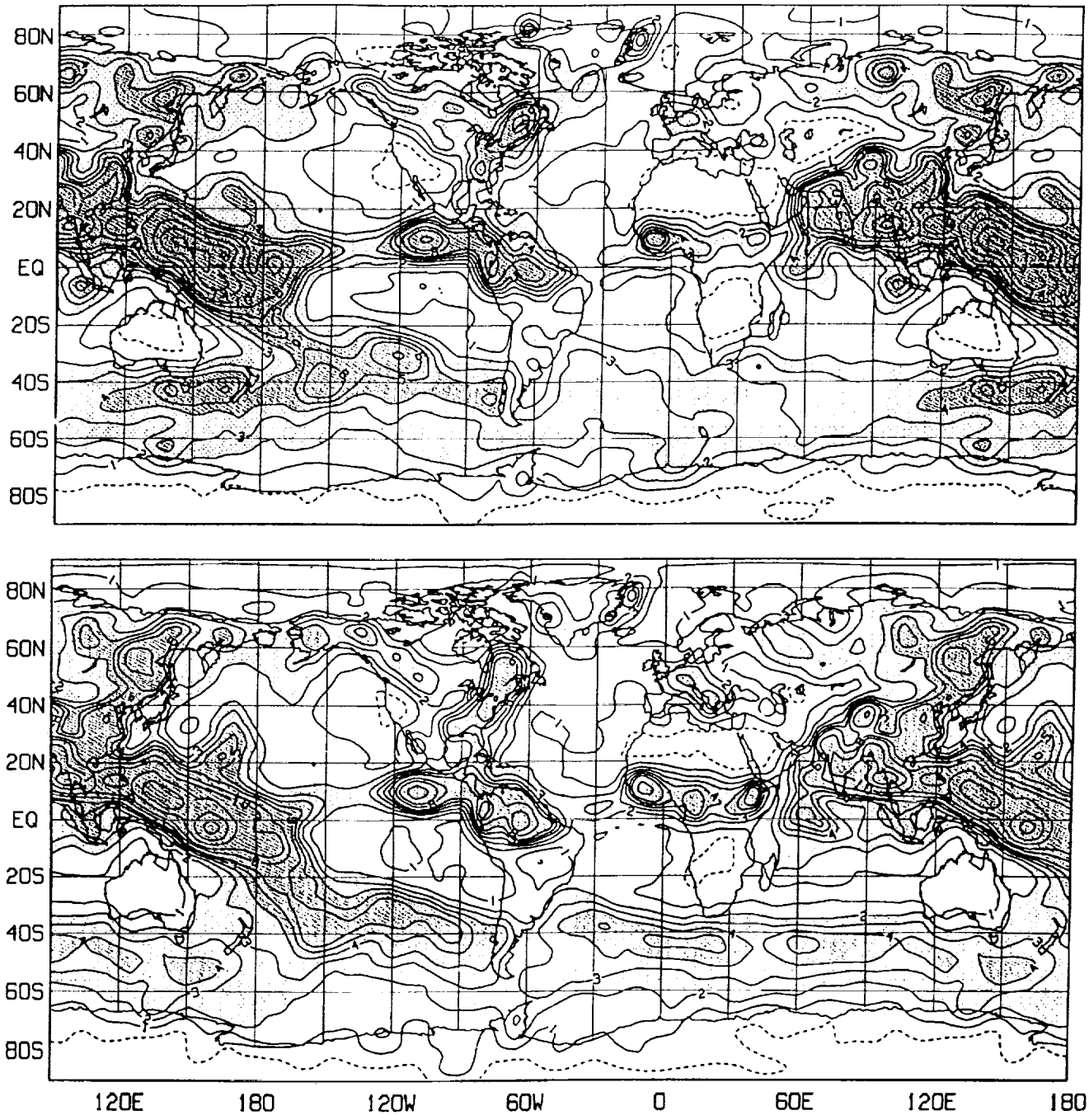

Figure 10a. Model simulated July precipitation in mm/day for a) normally wet land *(top)*, and b) initially wet land *(bottom)*. Soil moisture is interactive in both cases.

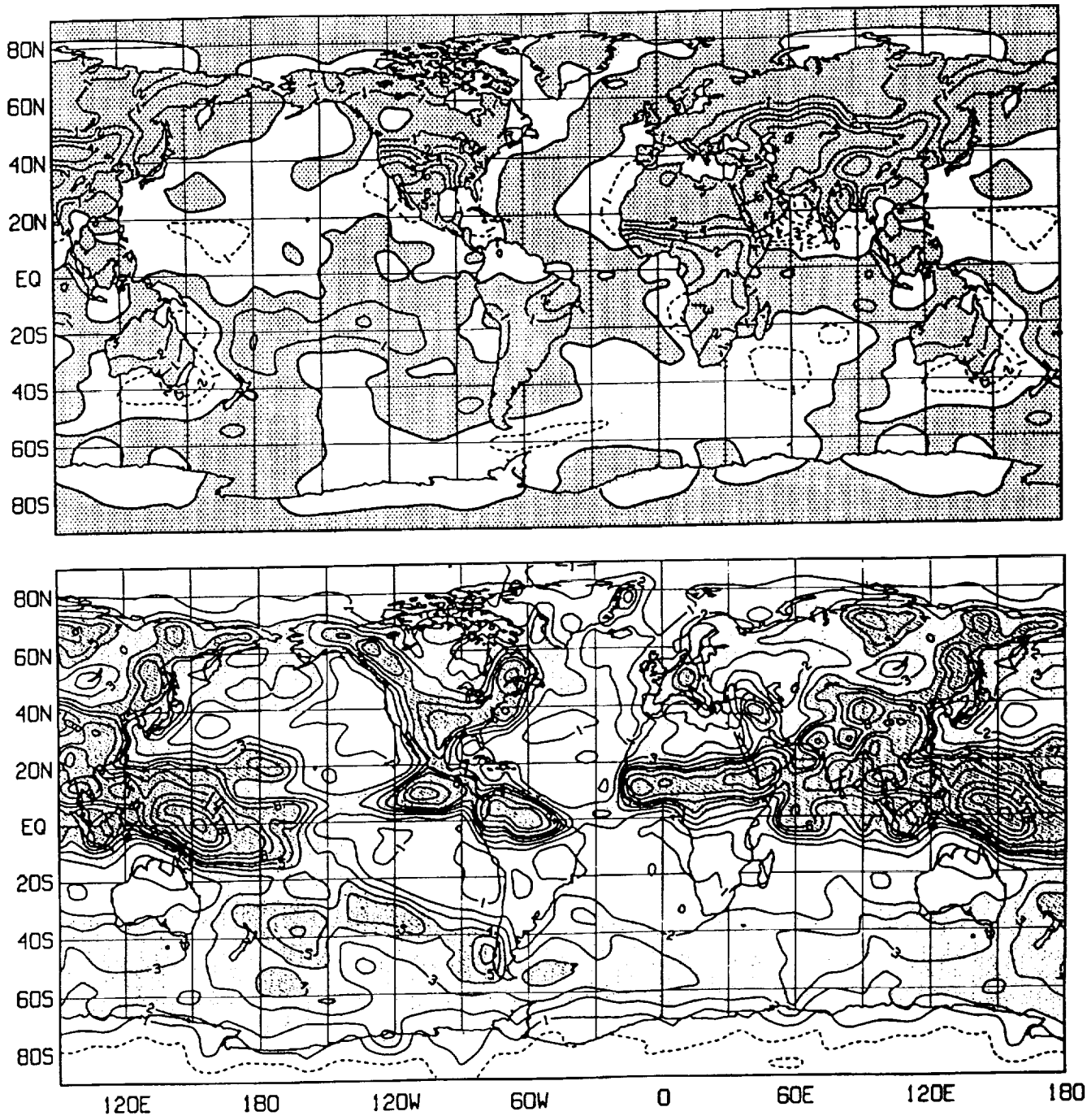

Figure 10b. For perpetually wet land, model simulated evaporation anomaly *(top)* and precipitation *(bottom)*. Both fields are in mm/day.

2.4 Land-Atmosphere Interaction Studies with SiB-GCM:

Several recent studies with the SiB-GCM have further enhanced our understanding of land-atmosphere interactions. The experiments were conducted to reinvestigate our understanding of the earth-atmosphere interactions using SiB. We describe the following experiments with the SiB-GCM.

a) Soil Moisture Influence Studies: Two sets of studies of the influence of soil moisture with the SiB-GCM are conducted. The same control run is used in each case which is made with the climatological initial soil moisture of Mintz and Serafini (1984) that is uniformly prescribed into all the three soil layers of SiB at the initial time. In the first experiment, the simulation starts with the saturated soil initially which evolves naturally thereafter in response to hydrologic processes of the interactive soil moisture. The results show that SiB simulations do not produce a large difference in rainfall between normally wet and initially saturated soil conditions, Fig. 10a. We have determined that this is the outcome of a short moisture retention time scale of sandy deserts and large semi-arid regions. In other words, SiB allows for the characteristic porosity of desert soils. In other words, these soils dry quickly by gravitational drainage in the SiB-GCM. Thus, the influence of wetting the sand, in the Sahara Desert for example, on evapotranspiration does not last beyond a few days: a time period in which the soil dries naturally; accordingly, the monthly differences in evaporation and/or precipitation produced by these two simulations are not very large, particularly for semi-arid and desert regions. See for example, the 30N latitude belt of the Saharan region in Fig 10a.

To determine if various other model improvements may have changed the model's atmospheric hydrological characteristics so drastically as to invalidate previous results of Shukla and Mintz (1982) and Sud and Fennessy (1984) and Sud and Smith (1985), we made another simulation in which the soil was forced to remain saturated throughout the integration period. This produced global rainfall patterns, Fig. 10b, that are similar to those produced in Shukla and Mintz (1982) simulations which were made with an earlier version of the GLAS GCM. It shows that the model's atmospheric characteristics, even after all the improvements, are not too different (with or without SiB), but the land-atmosphere interactions, with regionally varying soil water retention characteristic as well as evapotranspiration time scales for different biomes with a variety of rooting depths, have a significant effect on the outcome of the land-atmosphere interactions. Thus, SiB simulation studies have shown that the rainfall response of the real world can be quite

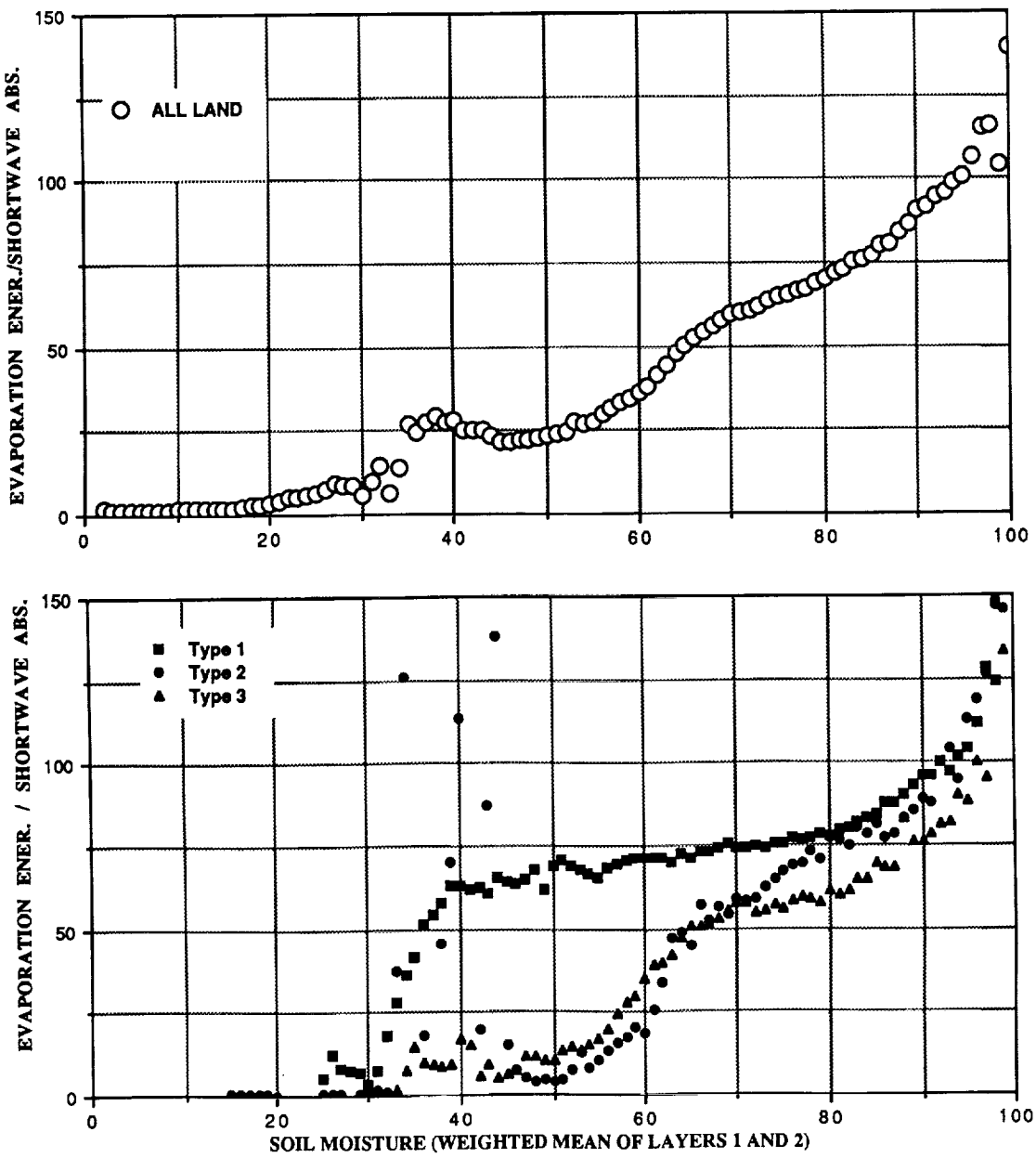

Figure 11. SiB-GCM-produced values of evapotranspiration divided by net solar absorption at the surface (a proxy for β-function) versus soil moisture. The data was binned into 100 soil moisture boxes of equal interval. The panels contain: *(Top)*: grand mean plots for all vegetation; and *(Bottom)*: results for three specific vegetation types representing Type-1: tropical forest; Type-2: broadleaf deciduous forest, and Type-3: mixed broadleaf deciduous and needleleaf evergreen forest.

different from that of the SSH-GCM, even if the soil moisture retention behavior of sandy soils is taken into account. The diurnal cycle of surface fluxes of the GCM with SiB shows that SiB evaporates more in response to increasing photosynthetically active radiation (PAR) as the sunshine increases, but a limiting value of evaporation is reached after which the evaporation either stays the same or actually reduces. Both effects are supported by observational data; however the latter is much too strong in the SiB on which Sellers et al. (personal communications, 1990) are currently working.

In Figure 11 we see SiB-GCM simulation of β-function inferred as a percentage of the solar energy fraction used for evaporation. It is plotted as a function of soil moisture in the two top layers which contain all soil layers up to the vegetation-root zone. Evidently, SiB produces virtually no evaporation for soil moisture less than 30%. The evaporation fraction increases thereafter but the its dependence on soil moisture is a strong function of vegetation type. The evaporation exceeds 100% of solar income at about 95% soil moisture; this is evidently a consequence of re-evaporation of intercepted rain by vegetation canopies, particularly forests, at the expense of sensible heat. We emphasize that such behavior is difficult to reproduce in a SSH-GCM. It is quite intriguing to note that the episodes of daily evaporation exceeding the solar radiation were few but mostly over eastern India. The circumstances involved cloudy conditions with very little solar radiation and strong winds producing evaporation at the expense of sensible heat. Moreover, if one were to address issues relating to improvement of the biosphere by land management (Anthes, 1984), the influence of changing land surface characteristics must be taken into consideration. There is a distinct possibility that such issues can be realistically addressed with the SiB-GCM.

b) Surface Roughness Influence Studies: Two July simulations, one with the surface roughness of the SSH-GCM and the other with the surface roughness of SiB-GCM were compared in this investigation. The drag coefficient and therefore the surface roughness in the former depends only on orography, which represents crudely a proxy for vegetation and terrain, whereas the surface roughness in the latter depends on vegetation height alone (Dorman and Sellers, 1989). The actual differences between these simulations were very complex and therefore it is evident that in order to isolate the role of surface roughness one needs to analyze the ensemble mean differences of several July simulations; however, it is possible to isolate crudely the effect of land-surface roughness on the surface stress in some regions. The Gobi Desert, north of the Himalayas, is a region of large surface roughness change. It has much larger surface roughness in the SSH-GCM

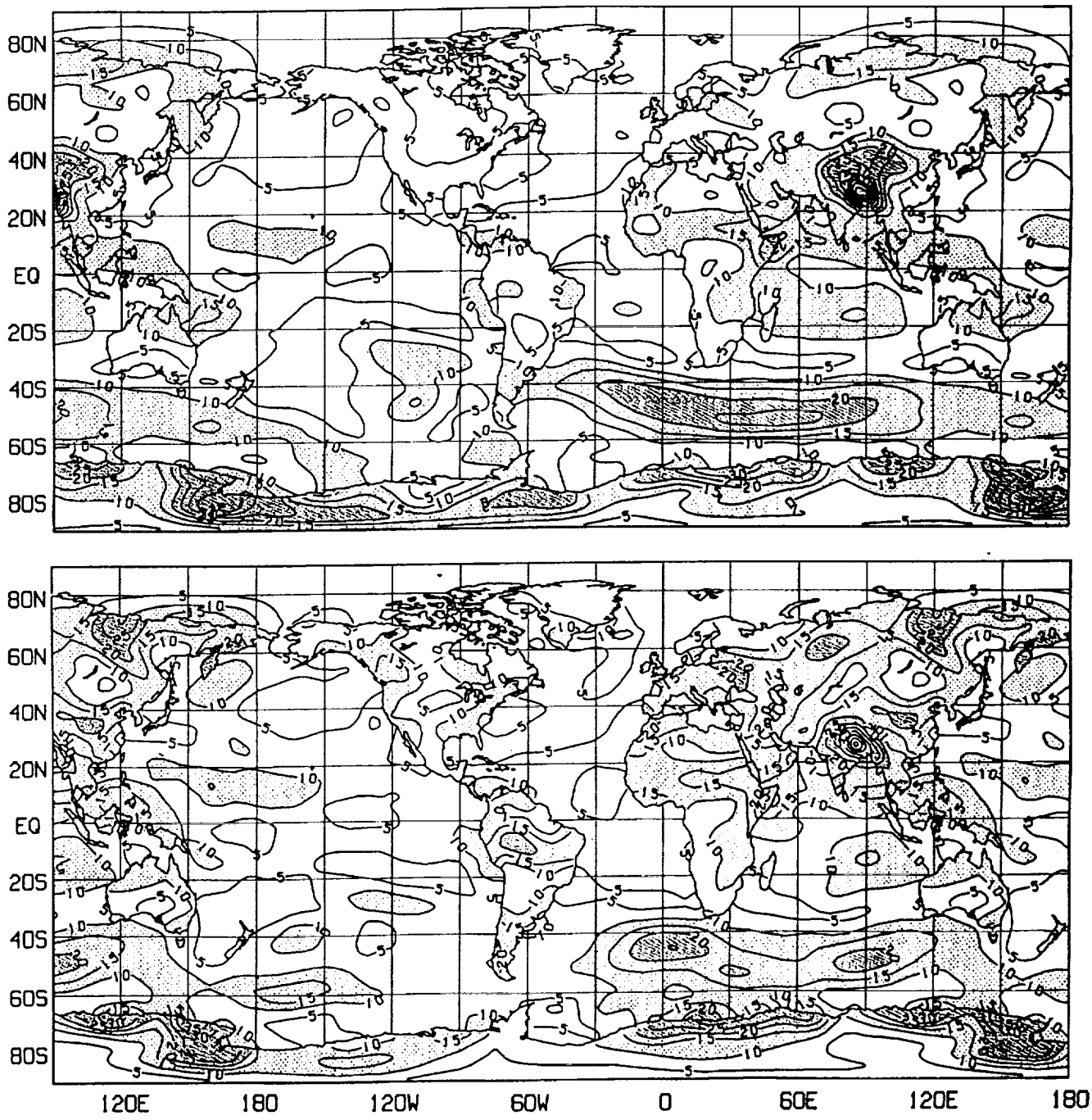

Figure 12. Surface stress in 0.01 N/m² for July simulation a) with land-roughness height of the previous model *(top)* and b) with vegetation-dependent roughness height from SiB *(bottom)*. Note large variability of surface stress over land for the latter simulation and large surface stress over the Himalayan mountain in the control case which calculates roughness of land as a function of geopotential height

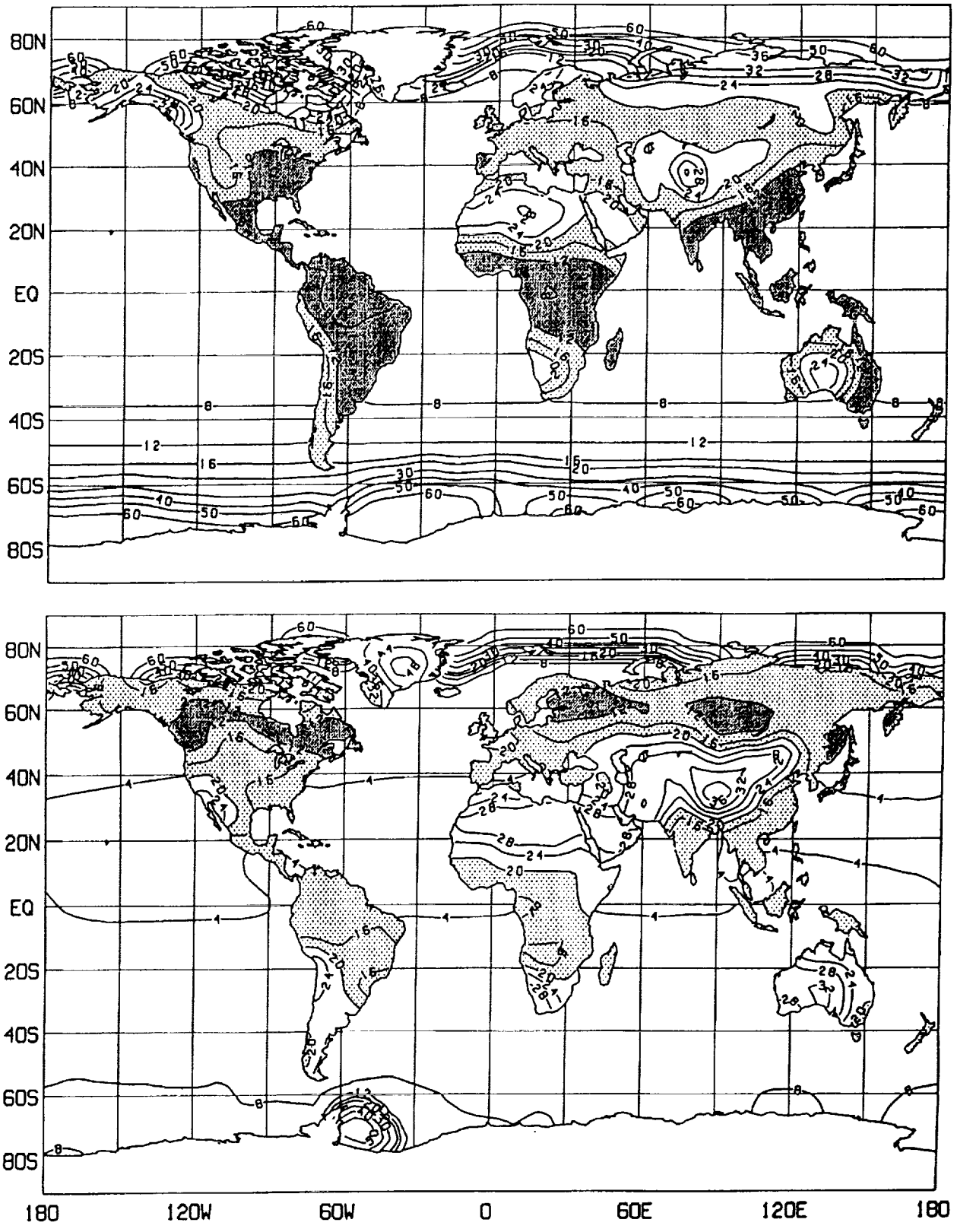

Figure 13. Surface albedo for an ensemble of July simulation a) as prescribed for the control case *(top)*, and b) vegetation-dependent surface albedo calculated within SiB from two-stream approximation *(bottom)*. Note larger land-surface albedo for SiB. For the control case, the surface albedo really holds for the visible part of the spectrum but it was applied to the entire solar income.

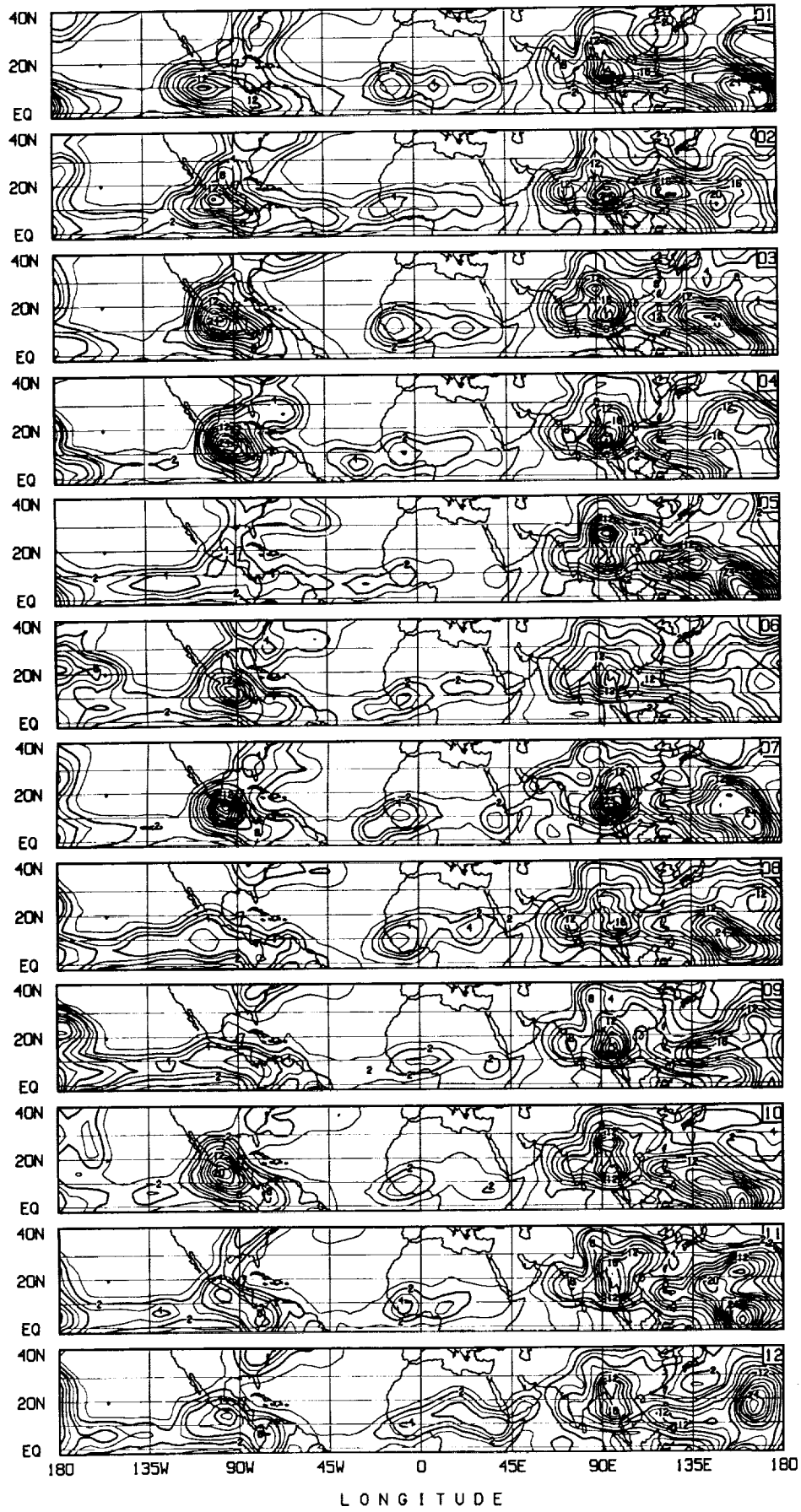

Figure 14a. Twelve consecutive maps of 30-day mean rainfall in mm/day produced by the perpetual July simulation with interactive soil moisture. Only the region from 0-40N is shown.

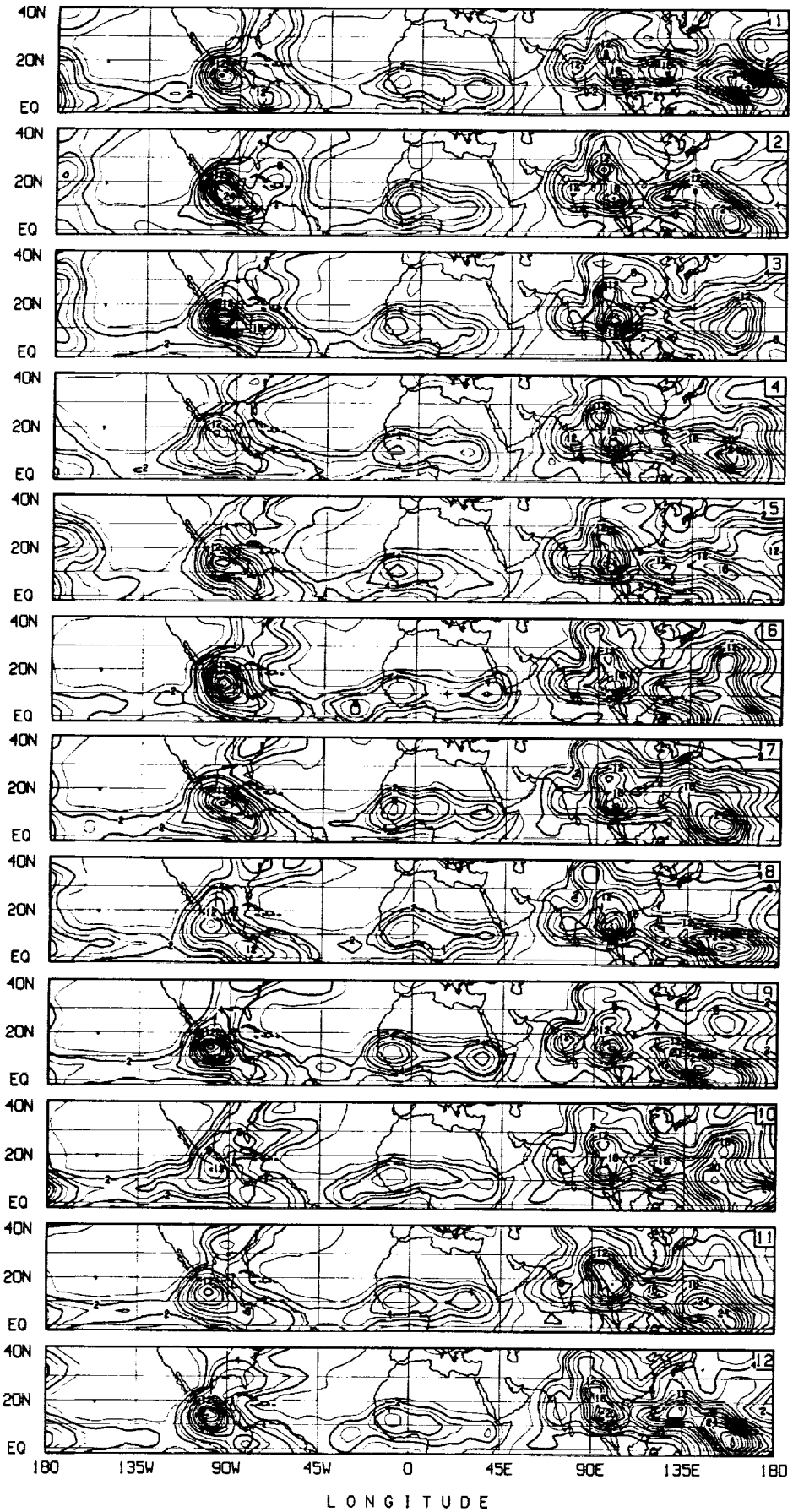

Figure 14b. Same as Fig. 14a, but for the climatologically prescribed soil moisture which was held constant throughout the integration.

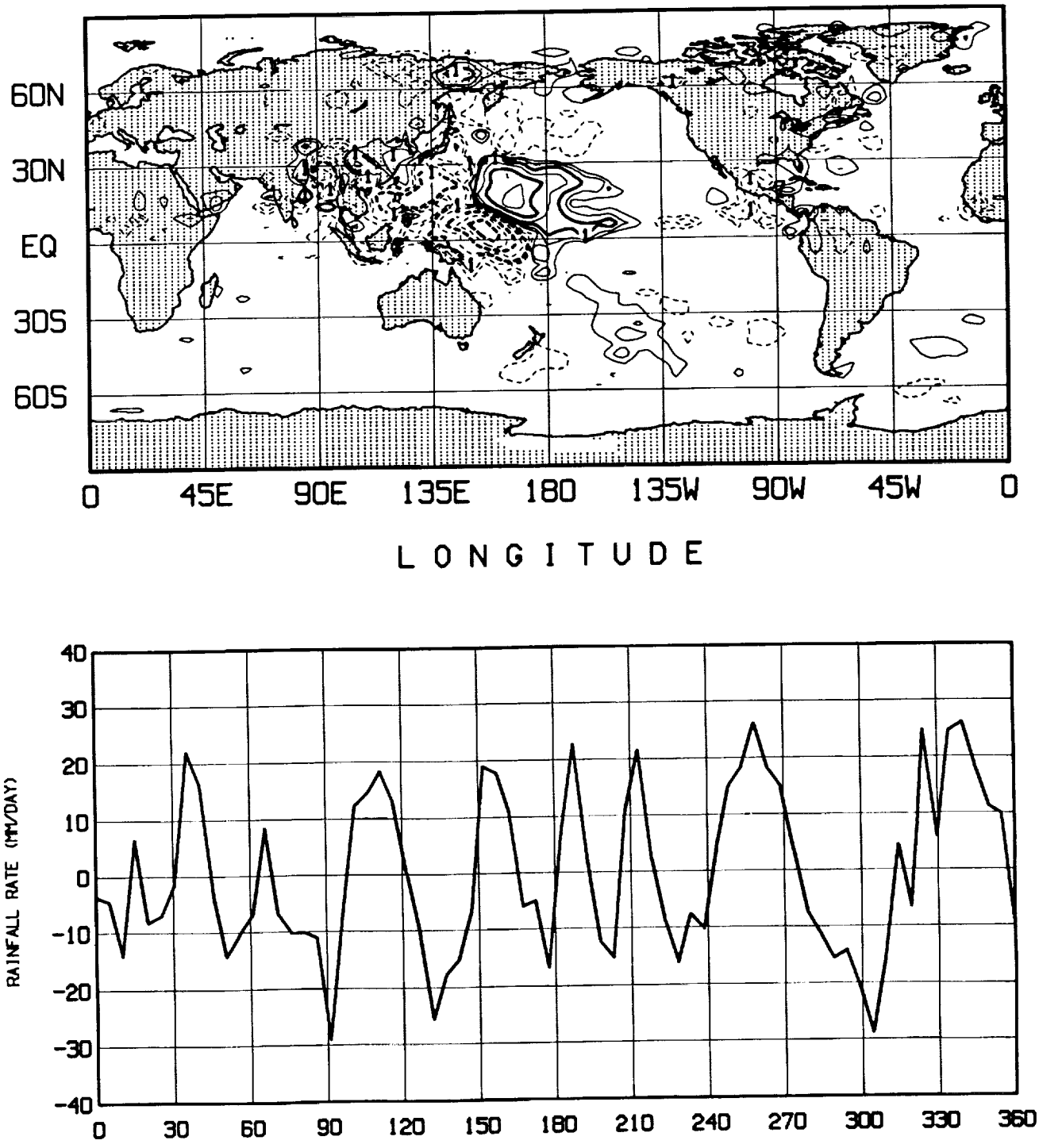

Figure 15a. Time series and pattern of the most dominant EOF for 14a. Time series represents the amplitude of rainfall fluctuations and the pattern represents the structure of the fluctuations on a non-dimensional scale (multiplication factor = 0.1). Contours are for 0.25, 0.5, 1.0, 2.0, 4.0, 6.0, and 8.0 values. Heavy contours show values 1, 4, and 8.

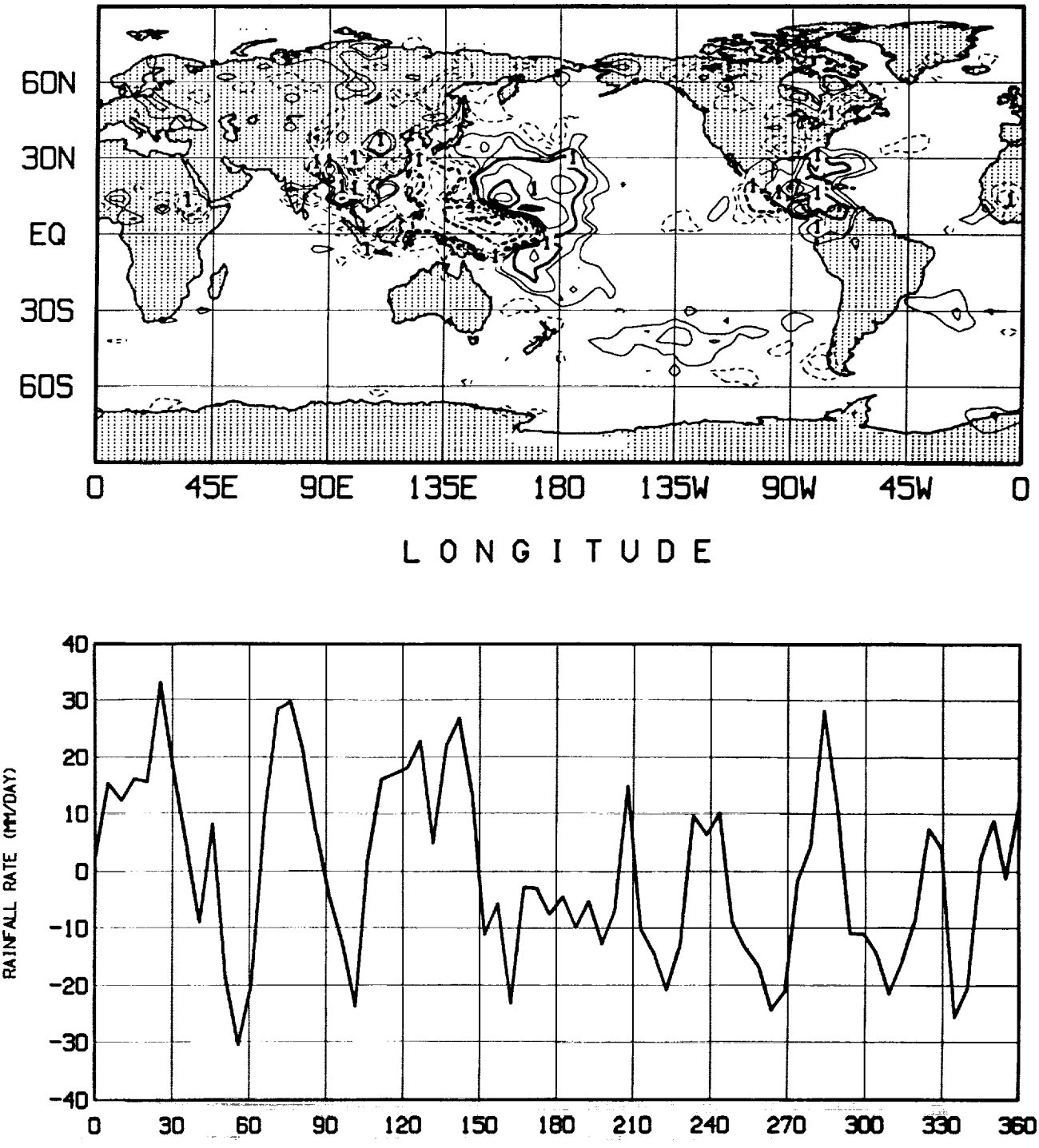

Figure 15b. Time series and pattern of the most dominant EOF for 14b. Figure details are the same as in 15a.

over India has very little variability particularly for fixed soil moisture simulation, whereas the precipitation has a large variability in the monthly means, (figure not shown). Such a variability is also found in the observations; see for example Hartmann and Michelson (1989). This indicates that the rainfall oscillations in the model may be realistic. It also suggests that the seasonal climate prediction problem is not merely a boundary forcing problem; to succeed, the slowly varying natural modes of the atmosphere, which can cover a large part of a season and which evolve to generate blocking highs and stationary long waves, must be accurately predicted by the model. An interesting spinoff of this research is that it may be possible to identify hydrologically unstable regions where an increase in evaporation produces a rainfall increase in excess of the corresponding evaporation increase. In such regions management of the biosphere can help significantly to change the local hydrologic cycle and climate.

Recently, Mehta (personal communications, 1990) performed empirical orthogonal function (EOF) analysis on rainfall, surface fluxes, outgoing longwave radiation (OLR), and wind data of the perpetual January and July simulations with the model. The internal consistency in the oscillations between wind and rainfall data is so remarkable that one can rule out the possibility of the oscillations emanating from random noise. The rainfall in the tropics exhibits 30- 40 day time scales in both simulations but with only a weak propagation of equatorial waves, (Figs. 15 a, b). The unrealistic singulation of tropical waves is partly understandable because they are difficult to capture in a coarse resolution model. However, existence of stationary 30-40 day characteristic time scales of atmospheric variability is a natural mode of the simulated system. Since this is also a well recognized time scale in the observations, we hope that model-produced vacillations are telling us something about the behavior of the real atmosphere. In a third perpetual July integration, the rainfall time series for the simulation with interactive soil moisture and 7% higher solar income which is consistent with solar radiation 9000 years ago, the dominant time scales of oscillation are found to be considerably longer. This result is quite different from the one in which normal solar radiation was prescribed. Thus, the comparison seems to suggest that the characteristic time scale can be modified by solar forcing.

2.5 Cloudiness and Radiative Effects of Clouds and Aerosols:

In the context of SiB-GCM, it is important to point out that the primary inputs to the SiB are rainfall, photosynthetically active radiation (PAR) and downward flux of

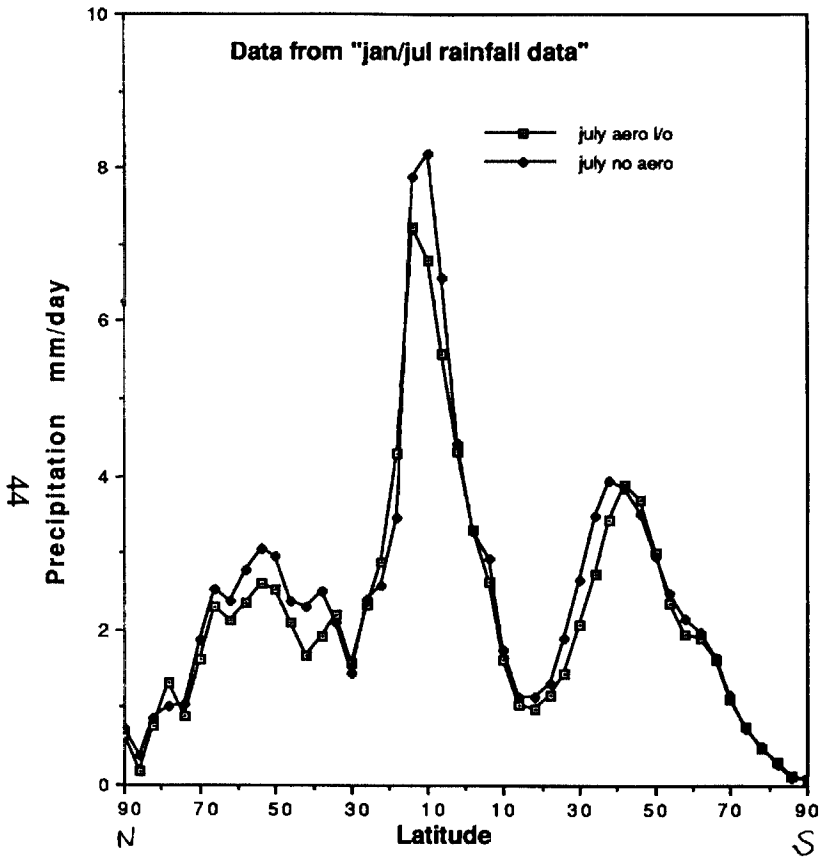

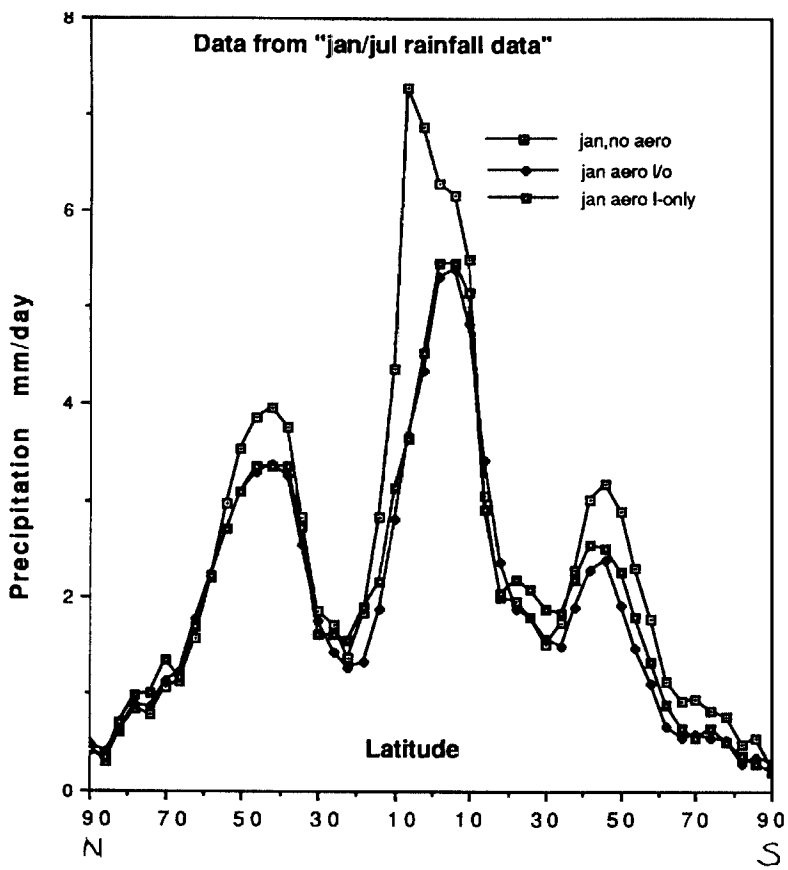

Figure 16. Influence of dust on the zonally symmetric rainfall in mm/day. Reduction in the tropical rainfall is most outstanding for both summer and winter simulations.

longwave radiation. For SiB we need four kinds of short wave fluxes: visible and near-visible fluxes of the beam and diffused forms. The shortwave radiation of the model had to be modified to make these fluxes interact with fractional clouds. Accordingly, the Lacis and Hansen (1974) radiation code was substantially modified. The current parameterization of solar radiation retains the Lacis and Hansen (1974) for absorption by ozone but contains the Chou (1986) parameterization for absorption by water vapor and dust . The original longwave radiation by Wu (1980) is still being used in the model; however, it was further modified by Wu (not published) to include the influence of fractional clouds which are now being produced dynamically. Currently, the influence of introducing fractional cloudiness is being systematically investigated.

In this section, we shall focus on the radiation balance at the surface of the earth. Clouds play a vital role in maintaining the observed radiation balance at the surface of the earth. Since the radiative transfer parameterizations, which include both the shortwave and longwave, must rely on the cloud parameterizations to provide them with fractional cloud distributions, as well as moisture and temperature soundings at all model levels, we need to ascertain that the model-produced cloudiness is realistic. Otherwise, excess or deficit solar radiation at the surface of land is bound to yield unrealistic surface fluxes. Some new and significant modifications to the cloud and cloud-radiation interaction parameterizations have been made in the GLA GCM. We include a short description of these changes for completeness of the discussion of our results.

a) Convective clouds: The GLA GCM produces convective, supersaturation and non-precipitating clouds using the predicted fields of temperature, specific humidity and winds. As discussed in section 3, the convective cloud calculation is an adaptation of the Arakawa-Schubert (1974) cumulus parameterization. In the process of producing cumulus rain, the Arakawa-Schubert scheme provides the mass of the detraining clouds for the life history of the cumulus convection episode which, in the context of the GLA GCM, is one half hour. By assuming conical shapes of the detraining cumulus anvils, the fractional cloudiness produced by the detraining cloud mass is obtained. Furthermore, the detraining cloud anvils at the center are assumed to be equal to the sigma layer thickness which linearly tapering off to zero at the edges of the cone. The primary advantage of these assumptions is that besides being roughly in accord with observations as well as schematic cloud pictures, identical cloud fractions for full and/or semi-conical cloud forms are produced. The fractional cloud cover determination is also useful for calculating the mass of rain water droplets per-unit-volume of the air. Following the

Marshall-Palmer (1948) drop size distribution for rain and assuming that all rain drops fall at their terminal velocity, the evaporation from falling rain is calculated according to the Sud and Molod (1988a, Appendix A) parameterization. Since, in nature, these clouds may last for periods far beyond the time period for convective showers, we include this effect by inferring the non-precipitating clouds from the relative humidity of a model layer following Slingo and Ritter (1985). The method is extremely simple and yet it yields a reasonable influence on the surface energy balance. Briefly, it is described below.

b) Supersaturation Clouds: Supersaturation (also called large-scale) clouds can appear at any sigma level of the model if the specific humidity at that level exceeds the saturation specific humidity. Clearly, then, all supersaturation clouds produce precipitation. These clouds are generated after the atmosphere has been adjusted by the convective clouds. However, all raindrops from convective as well as large-scale clouds evaporate in the atmosphere as they fall, using the same parameterization of Sud and Molod (1988a); the only difference being that the large-scale rain is taken to be spatially homogeneous whereas the convective rain, which appears below the cloudy region, is assumed to maintain the Ruprecht and Gray (1976) satellite-derived rainfall intensity distribution. Therefore, large-scale rain of small magnitudes may not reach the ground; alternatively, even for strong and intense rainfall, the atmospheric layers intercepted by the falling rain may not be saturated immediately. However, if the rain persists for a long time (4-10 hours, depending upon the intensity), near saturation conditions are produced by the scheme which is consistent with observations. Both of these effects are realistic and are in accord with observations.

c) Non-Precipitating Fractional Clouds: The fractional cloud cover, f_k, of non-precipitating clouds in any layer are inferred solely from the relative humidity of the layer following the empirical relation of Slingo and Ritter (1985):

$$f_k = \max\left[\left(\frac{RH_k - Crit_k}{1 - Crit_k}\right), 0\right] \qquad (1)$$

where the relative humidity at a sigma level k is given by RH_k; and its critical value, $Crit_k$, is also a function of k. For a sigma layer (σ_K), the critical relative humidity, $Crit_k$, is calculated from an empirical relation:

$$Crit_k = 1 - 2\sigma_k + 2\sigma_k^2 + \sqrt{3}\,\sigma_k\left(1 - 3\sigma_k + 2\sigma_k^2\right) \qquad (2)$$

These clouds are fractional in extent and interact with both the short and longwave radiation fluxes. The main advantage of the Slingo and Ritter parameterization is its simplicity and its ability to make a useful impact on the simulations of monthly surface radiation balance. In the GCM, the cloud fractions are calculated by both the Sud and Molod (1988) and Slingo and Ritter (1985) methods, and the higher value of cloud fraction is retained. In order to take full advantage of this seemingly simple fractional cloud parameterization, we had to adjust the fractional cloudiness by tuning the threshold relative humidity to produce about 50% global mean cloudiness.

d) Cloud-Radiation Interaction: The solar radiation absorbed by the atmosphere depends upon the cloudiness, surface albedo, water vapor and ozone concentrations of the atmosphere, and the solar zenith angle. Ozone absorbs primarily in the spectral region of wavelengths less than 0.69 μm, while water vapor absorbs in the near-infrared.

For a cloudy atmosphere, solar fluxes are computed using the multiple scattering scheme of Lacis and Hansen (1974). However, the scheme is not appropriate for a fractional cloud cover. In that case, an adjustment is made to the cloud optical thickness, τ. The physical basis being that an equivalent optical thickness, τ_e, can be found for any cloud fraction, f_c, such that if the cloud is smeared homogeneously throughout a sigma layer, it produces the same grid-averaged solar flux transmission, absorption and/or reflectance as by the partially cloudy layer. The following relation is derived by equating the sum of the model's shortwave radiation through the cloudy and clear fractions of the layer with that of the uniformly cloudy layer of equivalent optical thickness, τ_e:

$$\frac{\kappa\tau_e}{1.0 + \kappa\tau_e} = f_c\left(\frac{\kappa\tau}{1.0 + \kappa\tau}\right) \qquad (3)$$

The constant κ has a value of 0.13 for the parameterization in Lacis and Hansen (1974).

e) Influence of Aerosols: The influence of dust depends on its amount and radiative properties. The radiative properties consist of optical thickness, single scattering albedo,

and scattering asymmetry factor. The climatological values of these properties of dust, in our GCM, are based on the WMO data, (WCP-55, 1983). Without the absorption and reflection by dust aerosols, the model- simulated solar radiation at the surface of the land, particularly in dry, cloud-free desert regions, becomes too high. This leads to unrealistic vegetation-atmospheric interactions. Lack of shortwave absorption by the aerosols was also responsible for lower temperatures in the lower troposphere. Therefore we decided to include the climatological distribution of aerosols, as a first step. The calculation of optical thickness, $\overline{\tau}$, single scattering albedo, $\overline{\omega}$, and asymmetry factor, $\overline{g}$, for cloudy atmosphere with dust aerosols is calculated as follows:.

$$\overline{\tau} = \tau_{wv} + \tau_{cs} + \tau_{ca} + \tau_{ds} + \tau_{da} \tag{4}$$

$$\overline{g} = \frac{g_c(\tau_{cs} + \tau_{ca}) + g_d(\tau_{ds} + \tau_{da})}{(\tau_{cs} + \tau_{ca}) + (\tau_{ds} + \tau_{da})} \tag{5}$$

$$\overline{\omega} = \frac{(\tau_{cs} + \tau_{ds})}{(\overline{\tau})} \tag{6}$$

where, subscripts wv, cs, ca, ds, da represent water vapor, cloud scattering, cloud absorption, dust scattering, and dust absorption values, of the particular parameter. For the visible channels, water vapor optical thickness and cloud absorption optical thickness are negligible. In this way, the influence of dust-cloud-water vapor mixture is included consistently for the visible and infrared windows of the solar radiation. In the future, we will produce a dust lifting, transport and deposition model that includes dust scavenging by rain.

Currently, we are using much larger optical thicknesses for clouds than those proposed by Lacis and Hansen (1974). These values are about 2.5 times the earlier Lacis and Hansen values and are in better agreement with the values derived by Peng et al. (1982) using Fiegelson (1978) aircraft measurements of cloud properties. Moreover, these higher values of cloud albedos produce realistic planetary albedo for a fractionally cloudy atmosphere which has lower cloudiness, as compared to the previous version in which the entire grid-box was covered by clouds.

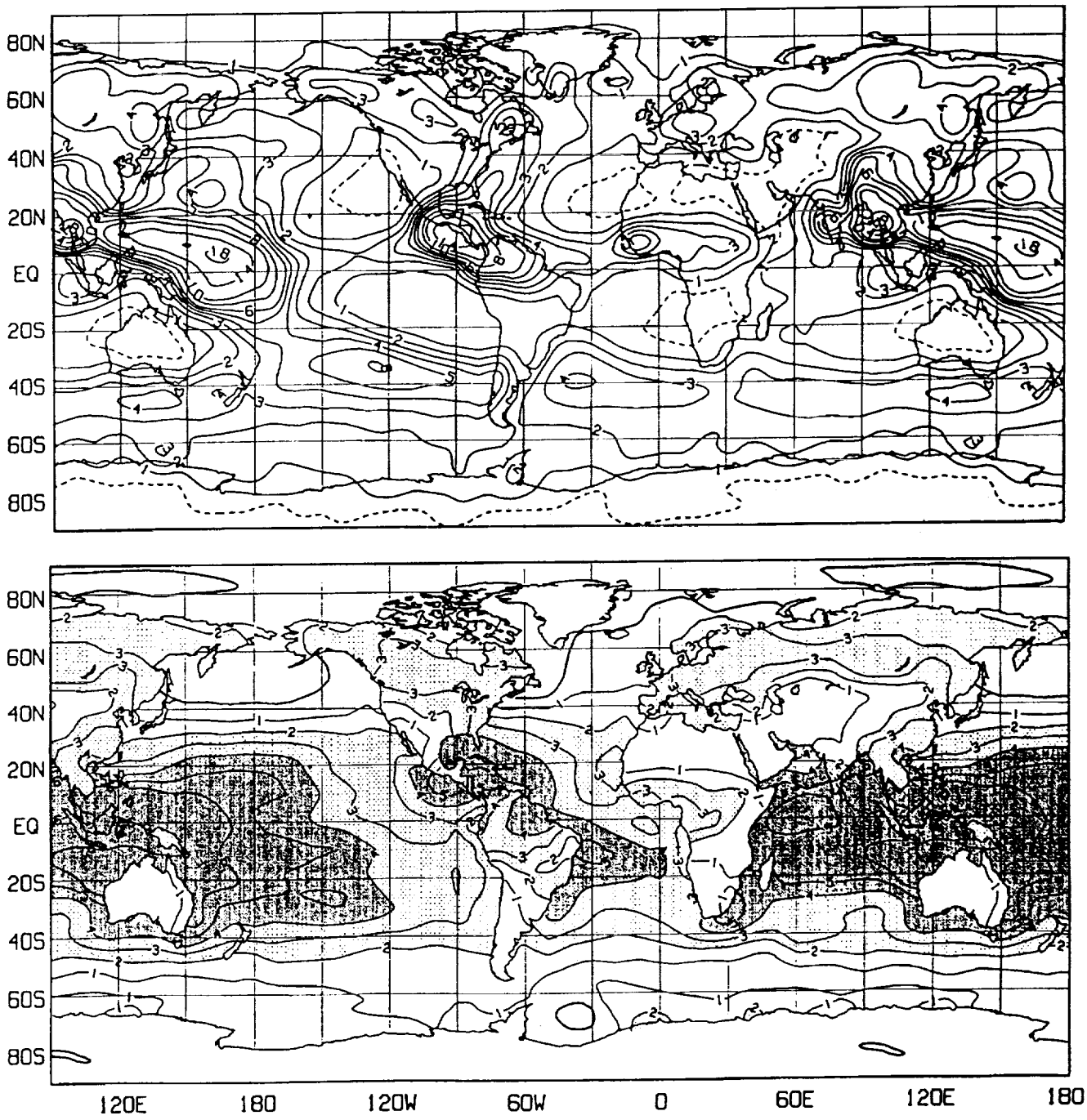

Figure 17. June-July-August simulation of: a) rainfall in mm/day *(top)*, and b) evaporation in mm/day *(bottom)*. Global mean: rainfall = 2.67 and evaporation = 2.70.

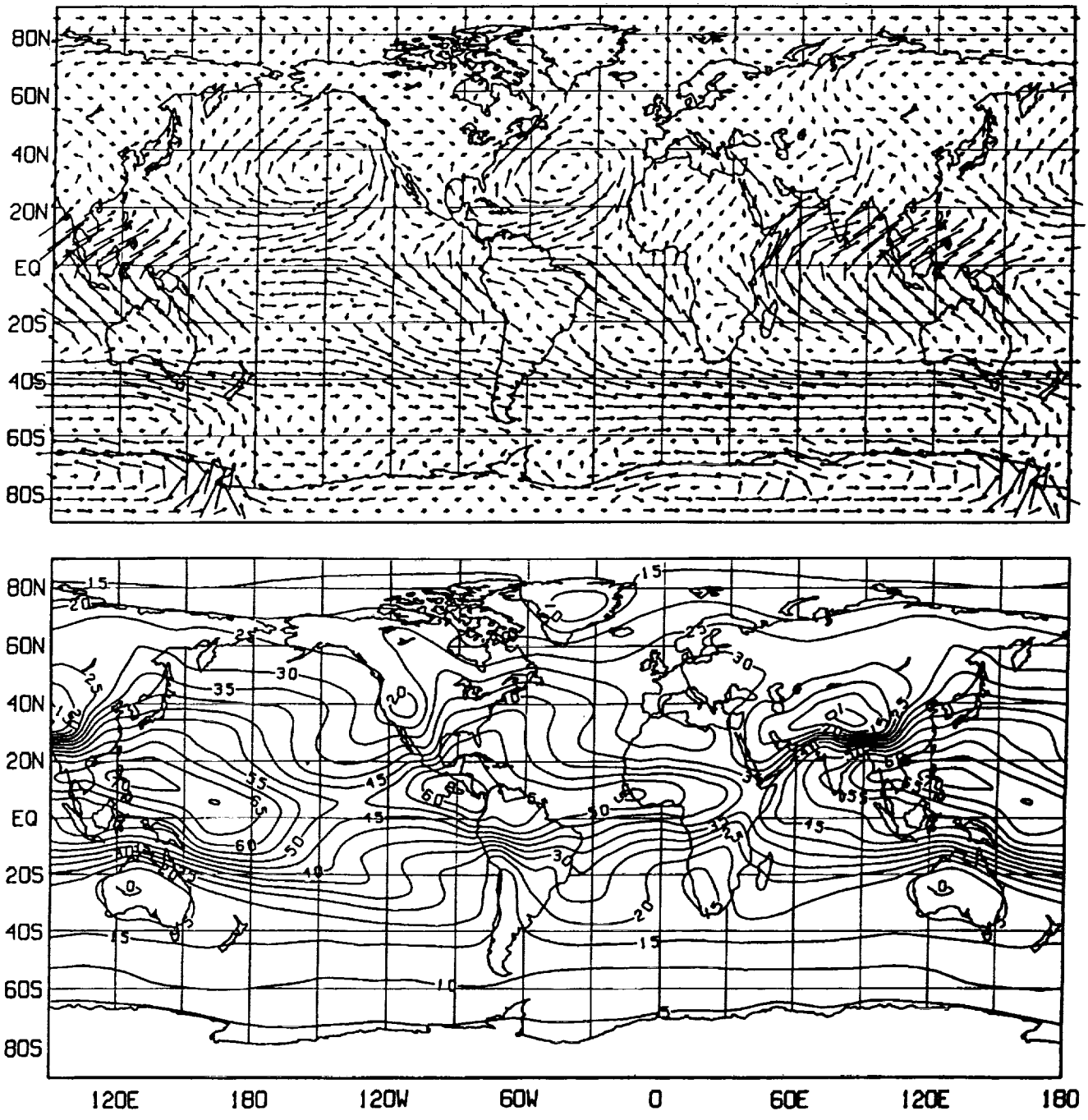

Figure 18. June-July-August simulation of: a) boundary layer winds *(top)* and b) mean precipitable water in mm *(bottom)*. Wind vectors: 10 m/sec = 15 deg. latitude. Global mean precipitable water = 30.5 mm.

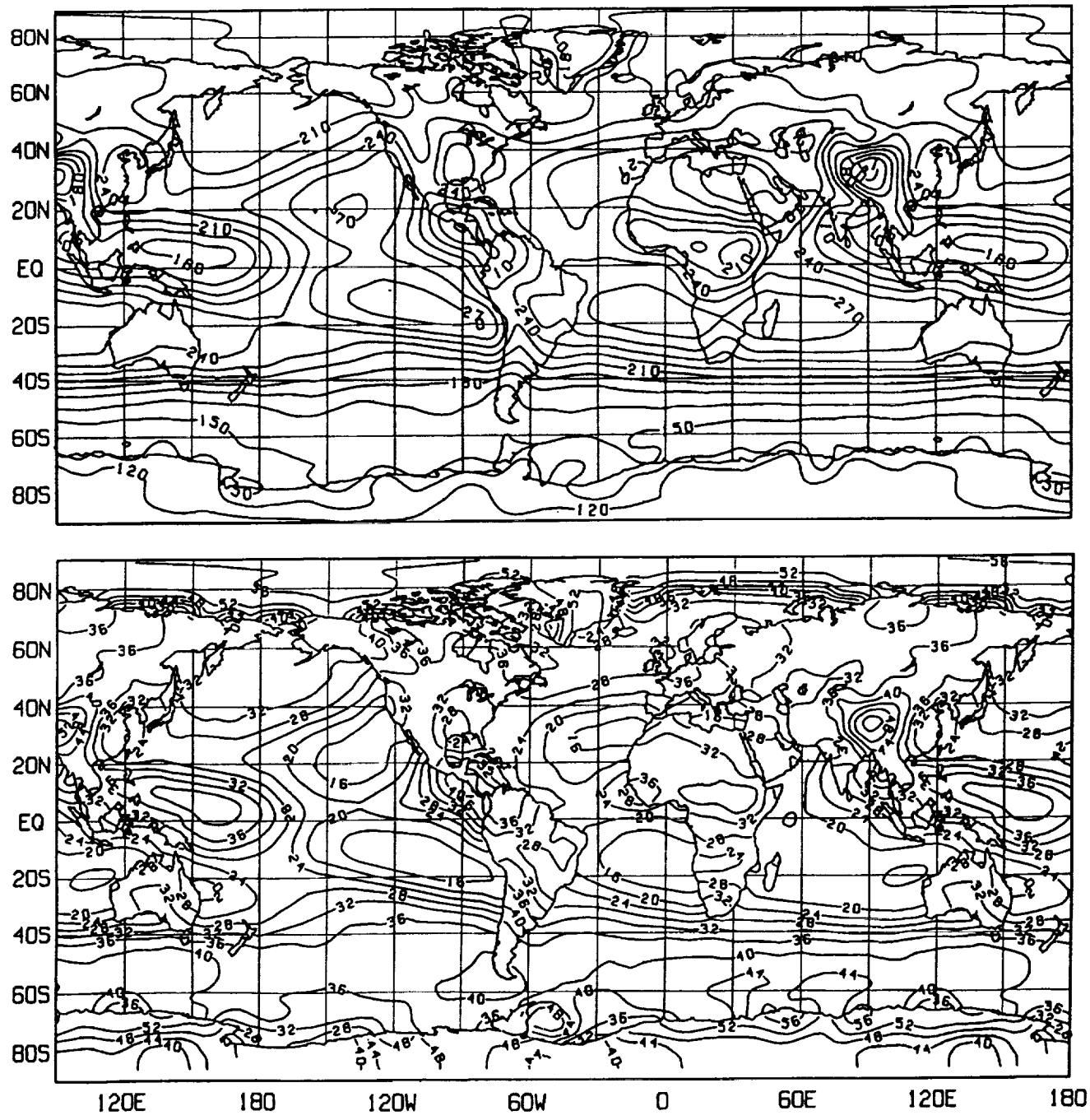

Figure 19. June-July-August simulation of: a) OLR in W/m² *(top)* and b) planetary albedo *(bottom)*. Global mean OLR = 220 W/m² and global mean planetary albedo = 28.9%.

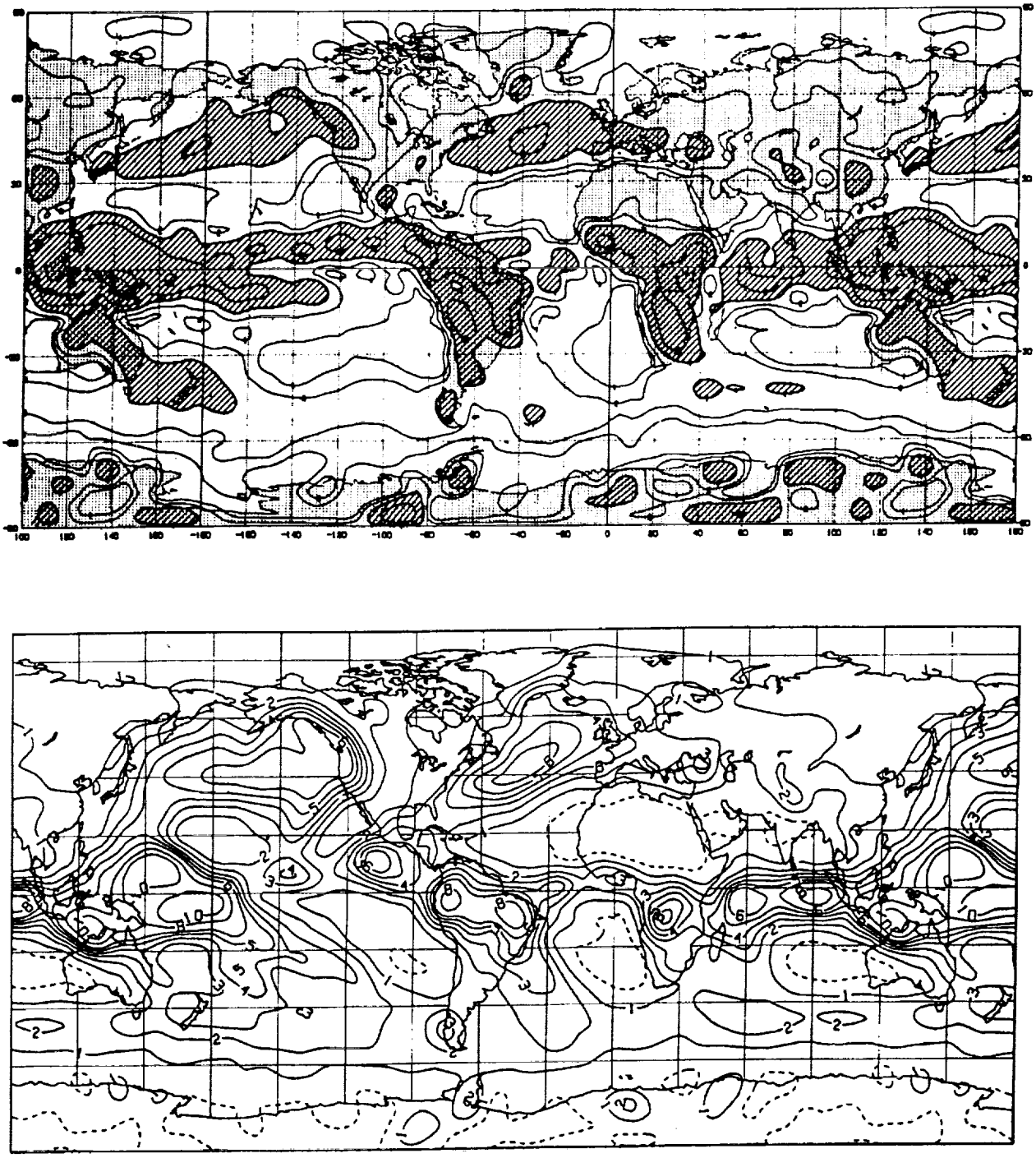

Figure 20a. A comparison of rainfall (mm/day) climatology of Kalnay et al. (1983) simulation with the current SiB-GCM simulations with all the modifications illustrated in the paper for January 1979. *Top:* Kalnay et al. (1983), and *bottom*: present model. (Rainfall contours above 4 mm/day are shaded.)

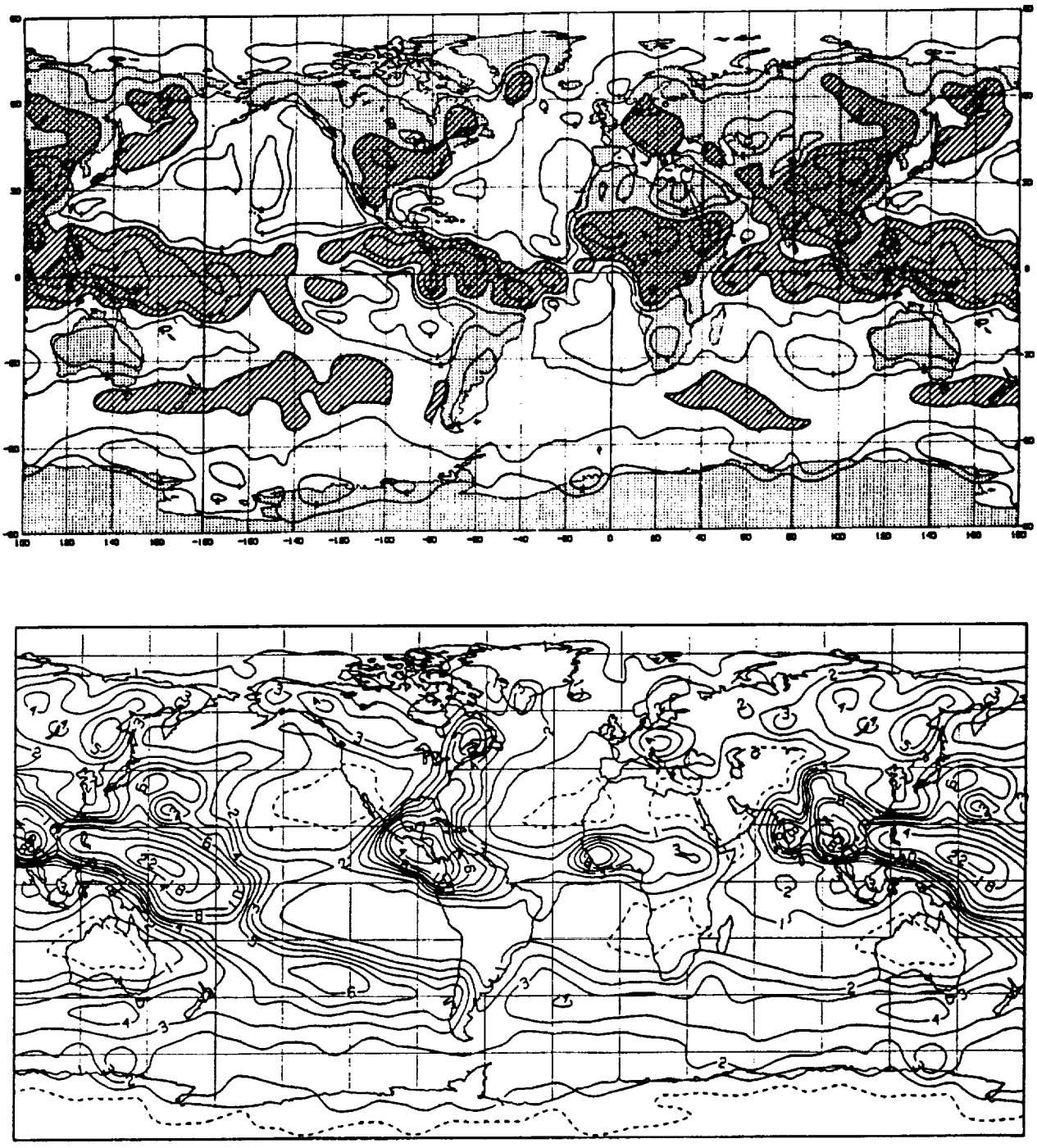

Figure 20b. Same as Fig. 20a, but for July 1979.

4. SUMMARY AND DISCUSSION

This article has assembled basic concepts, ideas and approaches which have led to several improvements in the physical parameterizations of the GLA GCM over the last 10 years. The relevant publications which contain details of the new parameterizations and an intercomparison of model simulation results have been duly referenced. One very serious question that plagues all the climate studies with models remains: how to delineate the understanding of the behavior of the real atmosphere from the understanding of the behavior (personality) of the model. Even though it is important to gain an insight into both, truly it is the understanding of the atmosphere that we are seeking; therefore, important to isolate one from the other. At present, we are unable to isolate these two components. We recognize that in a majority of case studies reported here, except for the SST anomaly influence simulations of the atmosphere for the recent El Niño events, the results are difficult tp validate against the observations. However, the basic gains from various model improvements and an inferred understanding of the global hydrologic cycle resulting from these studies is still quite useful and is summarized below:

i. Implementation of SiB into the GLA GCM followed by an assessment of the influence of vegetation on the surface fluxes of heat moisture and momentum in different regions of the world reveals that surface fluxes of the biosphere are very different from those of the slab soil hydrology model (SSH). By comparing simulated climatology of the SiB-GCM with that of the SSH-GCM and differentially diagnosing the physical interactions that have led to these improvements, a strong influence of vegetation on evaporation, precipitation and circulation (which affects the moisture transport convergence and hydrologic cycle directly) has been demonstrated.

ii. SiB-GCM simulations have helped us to reassess results of some of our earlier land-atmosphere interaction studies. With effects of vegetation and soil characteristics taken into consideration realistically, the role of soil moisture in different regions of the world is found to be quite different from that inferred with the SSH-GCM model. This is primarily due to evapotranspiration characteristics of different biomes together with drainage characteristics of different soils. On the other hand, the

role of surface roughness has become somewhat unclear in an experiment with the SiB-GCM as compared to earlier experiments by Sud and Smith (1985a,b) and Sud et al. (1988) with the SSH-GCM. In the SiB-GCM simulations, the influence of surface roughness turns out to be very complex debarring a simple interpretation which was indeed possible with the SSH-GCM.

It is found that a reduction in evaporation over land can produce thermal lows (highs), and accompanying convergence (divergence) over land (ocean); through dynamics, it even affects the region of the "roaring forties" in the Southern Hemisphere which have no direct influence of SiB on them. Excessive rainfall over Siberia was virtually ameliorated in response to reduced surface evaporation, whereas the monsoonal type of rainfall in the coastal regions of large continents was found to be related to the excessive radiation balance at the land surface.

iii. Some of our recent simulation studies have helped us better understand the biogeophysical component of desertification. In the Sahelian context, the primary mechanism which drives the rain-band southwards in the Sahel is the positive feedback effect of surface evaporation on northward propagation of the ITCZ. A reduction in evaporation dries the boundary-layer which is the primary source of moist air for the cumulus clouds. Without this moisture, the warm, dry air produces dry convection instead of moist (cumulus) convection. The dry convection helps mix the boundary-layer moisture into the sinking and diverging dry air aloft. In that way, dry convection provides the escape route for the moisture that solar heating helps bring into the region in summer. We have verified this mechanism by moisture transport calculations for model simulations as well as by analysis of observations.

Sud and Molod (1988a) have demonstrated that moisture mixing by dry convection over the Sahara Desert is a major mechanism which keeps the Sahara rain-free in the monsoon season. We hypothesize that by biosphere management, which protects the natural vegetation and helps it to thrive, the land evaporation of dry semi-arid regions can be enhanced. Such a change would keep the boundary-layer cool and moist, thereby

promoting moist convection instead of the dry convection in summer effectively altering the rainfall climatology of the region. The surface albedo feedback hypothesis is still valid, but the dry convective mixing turns out to be the primary process which keeps the Sahara rain-free in the summer months. The validity of this statement is evidentthat without dry convective mixing, the model begins to simulate rain in the Sahara Desert even if the highest observed surface albedo values for desert are prescribed. Nevertheless, it is reiterated that the positive feedback effect of surface albedo of deserts and desert border regions on the rainfall is still valid independently. The intention here is not to dispute those results or claims.

iv. We have made several investigations of the influence of physical parameterizations on the systematic drift in the simulated circulation and rainfall. The comparison of model simulations with observations and/or the analysis of observations revealed that the following two physical forcings directly bear on the hydrologic cycle: excessive drying and heating in the tropics, and excessive shortwave radiation at the surface of the earth with very strong thermally induced coastal convengence and rainfall in the summer (July) simulations. Model deficiencies specifically related to these were identified to be the specification of the critical cloud work function, cumulus entrainment parameter, λ, and cloud-radiation and aerosol-radiation interactions.

v The cumulus parameterization was found to be the primary determinant for the maintenance of tropical rainfall climatology. Having implemented the Arakawa-Schubert cumulus scheme, we made several modifications to it. We modified the specification of the critical cloud work function by requiring that the GCM-produced mean cloud work function agree well with the Marshall-Island soundings used by Lord (1978). Sud et al. (1990c) also experimented with the minimum limiting values of the cumulus entrainment parameter, λ_{min}, as introduced by Tokioka et al. (1988). These studies helped to adopt the Tokioka et al. (1988) recommendation for $\lambda_{min} = 0.0002 m^{-1}$. This change had a significant beneficial influence on the spinup problem and the monthly rainfall and circulation climatology of the model.

vi To improve the surface radiation balance we have recently included the climatological distribution of atmospheric aerosols. The aerosol density and radiative properties are taken from WMO recommendations. The combined effect of aerosols, clouds, and water-vapor was included by determining the equivalent optical thickness, single scattering albedo and asymmetry factor of the atmosphere. This modification produced much more realistic surface solar income. Globaly, the solar radiation absorbed at the surface reduced by about 20 W through its effect on evapotranspiration, which made a large positive impact on the rainfall climatology, particularly in tropics. All these improvements were made to the model in a series of sequential steps in which each subsequent step made the model somewhat better than before.

vii The perpetual July and January simulations, with and without interactive soil moisture, have helped us isolate the natural variability of the earth-atmosphere system. For the first time we have seen that monthly means of several quantities including the precipitation can fluctuate on a 30- 40 day time scale even without any changes in the boundary forcing. This result suggests that the 30-40 day mode is a characteristic time scale of the free atmospheric vacillations. A new finding in these simulations is the existence of a 60-90 day time scale in an interactive soil moisture run with 7% higher solar radiation. This indicates that solar heating of the earth-atmospheric system can modulate this time scale.

ACKNOWLEDGEMENTS

Both authors have gained significant insight into the behavior of the global hydrologic processes from discussions with Prof. Yale Mintz. Discussions with Dr. P. J. Sellers on Simple Biosphere-Atmosphere interactions were very valuable. Over the years, Dr. E. Kalnay and Prof. J. Shukla made many useful recommendations for analysis of studies summarized here. Drs. J. Pfaendtner, V. Mehta, and W. Chao and Technical Editors of GSCF provided useful comments on the original manuscript. Perpetual July and La Niña simulations for the 1988 U.S. drought were carried out in collaboration with Dr. K.-M. Lau. Dr. Ray Bates, Head of the Global Modeling and Simulation Branch, encourages this work and hopes to include the new parameterizations in the upcoming high-resolution version of the GLA GCM. Continued financial support by Dr. R. Murphy from the office of Land Programs of NASA Headquarters has been vital for this research.

REFERENCES:

Anthes, R. A. 1984: Enhancement of convective Precipitation by Mesoscale Variations in Vegetative cover in semi-arid regions Jour. Clim. and Appl. Meteorol. 23,541-54.

Arakawa, A., Y. Mintz, and A. Katayama, 1969: Parameterization of cumulus convection. Appendix 1, Numerical simulation of the general circulation of the atmosphere. Proc. WMO/IUGG Symposium on Numerical Weather Prediction, pp. Iv-7 to Iv-12.

_____, 1972: Design of the UCLA GCM, Numerical Simulation of Weather and Climate. Tech. Rep. No. 7, Dept. Meteorol., UCLA, Los Angeles California.

_____, and W. H. Schubert, 1974: Interaction of cumulus cloud ensemble with the large-scale environment, Part I. Jour. Atmos. Sci., 31, 674-701.

Atlas, R., 1987: The role of oceanic fluxes and initial data in the numerical prediction of intense coastal storms. Dyn. Atmos. Oceans, 10, 359-388.

_____, E. Kalnay, and M. Halem, 1985: Impact of satellite temperature sounding and wind data on numerical weather prediction. Opt. Eng., 24, 341-361.

Baker, W. E., R. Atlas, M. Halem and J. Susskind 1984: A case study of the forecast sensitivity to data and data analysis techniques. Mon. Wea. Rev., 112, 1544-1561.

Baker, W. E., 1983: Objective analysis and assimilation of observational data from FGGE. Mon. Wea. Rev., 111, 328-342.

Budyko M. I., 1958: Heat balance of the Earth's surface. Translated by N. A. Stepanova. Office of the Technical Service. U. S. Department of Commerce, Washington D. C.

Charney, J. G., 1975: Dynamics of deserts and rough in the Sahel. Quart. Jour. Roy. Met. Soc., 101, 193-202.

_____, W. J. Quirk, S. H. Chow, and J. Kornfield, 1977: A comparative study of the effects of albedo change on drought in semi-arid regions. Jour. Atmos. Sci., 34, 1366-1385.

Cheng, M.-D., 1989a: Effects of Downdrafts and mesoscale convective organizations on the heat and moisture budget of tropical cloud clusters. Part I: A diagnostic cumulus ensemble model. Jour. Atmos. Sci., 46, 1517-1538.

Cheng, M.-D., 1989b: Effects of Downdrafts and mesoscale convective organizations on the heat and moisture budget of tropical cloud clusters. Part II: Effect of meso-scale convective organizations. Jour. Atmos. Sci., 46, 1540-1564.

Cheng, M.-D., 1989c: Effects of Downdrafts and mesoscale convective organizations on the heat and moisture budget of tropical cloud clusters. Part III: Effect of convective scale downdrafts. Jour. Atmos. Sci., 46, 1566-1588.

Cheng, M.-D., and A. Arakawa, 1990: Inclusion of convective downdrafts in the Arakawa-Schubert cumulus parameterization. Department of Atmospheric Science. University of California, Los Angeles. pp 14

Chou, M.-D., 1986: Atmospheric solar heating rate in the water vapor bands. Jour. Atmos. Sci., 25, 1532-1542.

Crutcher, H. L., and D. M. Davis, 1969: U. S. Navy Marine Climatic Atlas of the World. Vol. VIII, The World. NAVAIR 50-1C-54. Naval Weather Service Command. Washington, D. C.

Cunnington, W. M., and P. R. Rowntree, 1986: Simulation of the Saharan Atmosphere-dependence soil-moisture and albedo. Jour. Roy. Meteorol. Soc., 113, 971-998.

Deardorff, J. W., 1972: Parameterization of the planetary boundary-layer for use in General Circulation Models. Mon. Wea. Rev., 100, 93-106.

Dickinson,R. E., A. Handerson-Sellers, P. Kennedy and M. F. Wilson, 1988: Biosphere-Atmosphere Transfer Scheme (BATS) for the NCAR Community Climate Model, NCAR Tech. Note. NCAR/Tn-275+STR. Boulder, CO, pp 69.

_____, A. Handerson-Sellers, 1988: Modelling Tropical Deforestation: A study of GCM land parameterization. Quat. Jour. Roy. Met. Soc., Vol. 114, 439-462

Donner, L. J., 1988 : An initialization of cumulus convection in Numerical Weather Prediction Models. Mon. Wea. Rev., 116, 377-85.

Donner, L. J. and P. J. Rasch 1989 : Cumulus initialization in a global model for Numerical Weather Prediction. Mon. Wea. Rev., 117, 2654-2671.

Dorman, J. L., and P. J. Sellers, 1989: A global climatology of albedo, roughness length and stomatal resistance for atmospheric General Circulation Models as represented by the simple biosphere model (SiB). Jour. Appl. Met. (in press).

Folland, C. K., T. N. Palmer and D. E. Parker, 1986: Sahel rainfall and worldwide sea temperatures 1901-85. Nature, 320: 602-607.

Feigelson, E. M., 1978: Preliminary radiation model of a cloudy atmosphere. Part I- Structure of clouds and solar radiation. Beit. Phys. Atmos., 51, 203-229.

Geller, M. A., Y. C. Sud, H. M. Helfand and K. Takano, 1988: Sensitivity of climatic response in a GCM to the selection of a cumulus scheme. Tropical Rainfall Measurements, (Eds.) John S. Theon and Nobuyoshi Fugono, Deepak Publishing, Science and Technology Corporation, Hampton Virginia, pp 57-67.

Hartmann, D. L., and M. L. Michelsen, 1989: Intraseasonal periodicities in Indian rainfall. Jour. Atmos. Sci., 46, 18, 2838-2862.

Henderson-Sellers, A. and Gornitz, V., 1984: Possible climatic impacts of land cover transformations, with particular emphasis on tropical deforestation. Climatic Change, 6, 231-257.

Jaeger, L., 1976: Monatskarten des Niederschlags fur die ganze Erde", Berichte des Dutschen Wetterdienstes, 18, No. 139. Im Selbstverlag des Duetschen Wetterdienstes, Offenbach, West Germany.

Kalnay, E., R. Balgovind, W. Chao, D. Edelmann, J. Pfaendtner, L. Takacs and K. Takano, 1983: Documentation of the GLAS fourth-order general circulation model. Volume I., NASA Tech. Memo. 86064, NASA Goddard Space Flight Center, Greenbelt, Maryland 20771.

_____, R. Atlas, W. Baker, and J. Susskind, 1985: GLAS experiments on the impact of FGGE satellite data on numerical weather prediction. Proceedings of the first National Workshop on the Global Weather Experiment, Vol. 2, PART-I, p 121-145, National Academy Press, Washington DC.

Krishnamurthy, V., 1982: The documentation of the Wu-Kaplan radiation Parameterization. NASA Tech. Memo. 83926. Laboratory for Atmospheric Science, Modeling and Simulation Facility, NASA. Goddard Space Flight Center, Greenbelt, Maryland 20771.

Krishnamurti, T. N., K. Ingles, S. Cooke, T. Kitade, and R. Pasch, 1984: Details of low latitude medium-range numerical weather prediction using a global spectral model. Part II: Effect of orography and physical initialization. Jour. Meteor. Soc. Japan, 62, 613-648.

Kuo, H. L., 1974: Further studies of the parameterization of the influence of cumulus convection on large-scale flows. Jour. Atmos. Sci., 31, 1232-40.

Lacis, A. and J. E. Hansen, 1974: A parameterization for the absorption of solar radiation in the earth's atmosphere Jour. Atmos. Sci., 31, 118-133.

Lau, K. M. and P. H. Chan, 1988: Intra-seasonal and Intra-annual variation of tropical convection: A possible link between the 40-50 day oscillation and ENSO. Jour. Atmos. Sci., 45, 506-521.

_____, and S. Shen, 1988: On the dynamics of intraseasonal oscillation and ENSO. Jour. Atmos. Sci., 45, 1781-1797.

Laval, K., 1983: GCM experiments with surface albedo changes. Paper presented at Third International School of Climatology, Erice, Italy, October 1983.

_____, and Picon, L., 1986: Effect of change of surface albedo of the Sahel on Climate. Jour. Atmos. Sci., 43, pp 2416-29.

Lean, J. and D. A. Warrilow, 1989: Climatic impact of Amazon Deforestation. Internal Report No. DCTN 79. Meteorological Office (Met. O. 20), London Road, Bracknell Berkshire RG12 2SZ.

Legates, D. R., and C. J. Willmott, 1990: Mean seasonal and spatial variability in global precipitation, International. Jour. Climatol., 10, 111-127.

Lord, S,. J. , 1978 : Development and observational verification of a cumulus cloud parameterization. Ph D. dissertation, Department of Meteor., University of California, Los Angeles. p 359.

Lord, S. J., W. C. Chao, and A. Arakawa, 1982: Interaction of a cumulus cloud ensemble with the large-scale environment. Part IV: The discrete model. Jour. Atmos. Sci., 39, 104-113.

Manabe,, S., 1969: The atmospheric circulation and hydrology of the Earth's surface. Mon. Wea. Review, 97, 739-74.

Marshall, J. S., and W. M. Palmer, 1948: The distribution of rain drops with size. Jour. Meteor., 5, 165-66.

Mintz, Y., P. J. Sellers, and C. J. Willmott, 1983: On the Design of an Interactive Biosphere for the GLAS General Circulation Model, NASA Tech. Memo. 84973, p 57, Goddard Space Flight Center, Greenbelt, MD 20771.

_____, 1984: The sensitivity of numerically simulated climates to land surface boundary conditions. J. T. Houghton (ed.), The Global Climate, Cambridge University Press, London, pp 70-105.

_____, and Y. Serafini, 1984: Global fields of normal monthly soil moisture, as derived from observed precipitation and an estimated potential evapotranspiration. Part V, Final Scientific Report Under NASA Grant No. NAS5-26, Dept. Meteorology, University of Maryland, College Park, MD. 20742.

Peng, Li, M.-D. Chou, and A. Arking, 1982: Climate studies with a multi-layer energy balance model, Part-I: Model description and sensitivity to solar constant. Jour. Atmos. Sci., 39, 2639-2656.

Posey, J. W., and P. F. Clapp, 1964: Global distribution of normal surface albedo. Geophysical International, 4(1), 33-48.

Randall, D. A., 1982: Monthly and seasonal simulations with the GLAS Climate Model, Proceedings of the Workshop on Inter-comparison of Large Scale Models used for Extended Range Forecast. European Centre for Medium Range Weather Forecast, Reading, England, pp. 107-66.

Reed, R. J. and E. E. Recker, 1971: Structure and properties of synoptic-scale wave disturbances in the equatorial western Pacific. Jour. Atmos. Sci., 28, 1117-1133.

Reynolds, R. W., 1988: Real-time sea surface temperature analysis. Jour. of Climate, 1, 75-86.

Reynolds, R. W. and W. H. Gemmill, 1984: An objective global monthly mean sea surface temperature analysis. Tropical Ocean-Atmosphere Newsletter, No. 23, 14-15.

Ruprecht, E., and W. M. Gray, 1976: Analysis of satellite observed tropical cloud clusters II thermal moisture and precipitation fields. Tellus, 28, 414-426.

Sato, N., P. J. Sellers, D. A. Randall, E. K. Schneider, J. Shukla, J. L. Kinter III, Y. T. Hou and E. Albertazzi, 1989: Effect of implementing the simple biosphere model (SiB) in a general circulation model. Jour. Atmos. Sci. , 46, 18, 2757-2782.

Salstein, D. A., R. D. Rosen, W. E. Baker and E. Kalnay, 1987: Impact of satellite based data on FGGE general circulation statistics. Quart. Jour. Roy. Meteorol. Soc., 113, 255-277.

Sellers, P. J., 1985: Canopy reflectance, photosynthesis and transpiration. In. Jour. Rem. Sens., 6(8), 1335-1372.

_____, Y. Mintz, Y. C. Sud, A. Dalcher, 1986: A simple biosphere model (SiB) for use within general circulation models. Jour. Atmos. Sci., 43, 505-531.

_____,1987: Modeling effects of vegetation on climate. *The Geophysics of Amazonia*. Eds: R. E. Dickinson, John Wiley and Sons, New York, New York, pp 244-64.

Shukla, J. , and Mintz, Y., 1982: The influence of land surface evapotranspiration on earth's climate. Science, 215, 1498-1501.

_____, C. Nobre and P. Sellers., 1989: Amazonia Deforestation and Climate Change. Manuscript prepared for publication in Science, October 1989.

Simpson, J., 1971: On cumulus entrainment and one dimensional models. Jour. Atmos. Sci., 28, 449-455.

Slingo, J. and B. Ritter, 1985: Cloud prediction in the ECMWF model. Tech. Rep. No. 46. European Centre for Medium Range Weather Forecasting, Reading, England.

Sommerville, R. C. J., P. H. Stone, M. Halem, J. E. Hansen, J. S. Hogan, L. M. Druyan, G. Russell, A. A. Lacis, W. J. Quirk and J. Tenenbaum, 1974: The GISS model of the global atmosphere. Jour. Atmos. Sci., 31, 84-117.

Sud, Y. C. and J. Abeles, 1980: A non-iterative calculation for the surface temperature and surface fluxes in the GLAS GCM. NASA Tech. Memo 80650. GSFC, Greenbelt, Maryland.

_____, and M. J. Fennessy, 1982: A study of the influence of surface albedo on July circulation in semi-arid regions using the GLAS GCM. Jour. Climatol., 2, 105-125.

_____, and M. J. Fennessy, 1984: A numerical study of the influence of evaporation in semi-Arid regions on the July circulation. Jour. Climatol., 4, 383-98.

_____, and W. E. Smith, 1984: Ensemble formulation of surface fluxes and improvement in evapotranspiration and cloud parameterizations in a GCM Boundary-Layer Meteorol., 29, 185-210.

_____, and W. E. Smith, 1985a: The influence of surface roughness of deserts on the July circulation: A numerical study. Boundary-Layer Meteorol., 4, 383-398.

_____, and W. E. Smith, 1985b: Influence of local land surface processes on the Indian Monsoon: a numerical study. Jour. Clim. and Appl. Meteor., 24, 1015-36.

_____, G. K. Walker, and W. E. Smith, 1988a: An analysis of sea-surface temperature anomaly simulation of atmospheric circulation for the winter of 1982-83. Modelling the sensitivity and variations of the ocean-atmosphere system. Report of a Workshop at the European Centre for Medium Range Weather Forecasting (11-13 May, 1988). pp 45-76.

_____, J. Shukla and Y. Mintz, 1988b: Influence of land surface roughness on atmospheric circulation and rainfall: A sensitivity study with a general circulation model. Jour. Appl. Meteor., 27, 1036-1054.

_____, and A. Molod, 1988a: The roles of dry convection, and cloud radiation feedback processes and the Influence of recent improvements in the parameterization of convection in the GLA GCM on circulation and rainfall Mon. Wea. Rev. 116, 2366-87.

_____, and A. Molod, 1988b: A GCM simulation study of the influence of Saharan Evapotranspiration and Surface-Albedo anomalies on July circulation and rainfall. Mon. Wea. Rev.,116, 2388-2400.

_____, W. C. Chao and G. K. Walker, 1989: Contributions to the implementation of Arakawa-Schubert cumulus parameterization in the GLA GCM. Fifth Conference on Weather Analysis and Forecast. Naval Postgraduate School, Monterey California. October 2-6, 1989.

_____, P. J. Sellers, Y. Mintz, M. D. Chou, G. K. Walker, W. E. Smith , 1990a: Influence of the Biosphere on the Global Circulation and Hydrologic Cycle- a GCM simulation Experiment. Agricultural and Forest Meteorology, 52, 1-2, pp. 133-179.

_____, K. -M. Lau, G. K. Walker, 1990b: Simulation of 1988 drought over North America. Paper presented at the 1988 US Drought Workshop at the University of Maryland. (to appear in the Workshop Proceedings, April 30-May,2 1990.).

_____, W. Chao and G. K. Walker,1990c: Contributions to the Implementation of Arakawa-Schubert Cumulus Parameterization in the GLA GCM. Jour. Amos. Sci., (in review).

Susskind, J., J. Rosenfield, D. Reuter and M. T. Chahine, 1984: Remote sensing of weather and climate parameters from HIRS/MSU on TIROS-N. Jour. Geo. Res. 89D, 4657-4676.

_____, D. Reuter and M. T. Chahine, 1986: Cloud fields retrieved from HIRS@/MSU sounding data. Jour. Geophys. Res.

Tiedtke, M. 1984: The effect of penetrative cumulus convection on the large-scale flow in a general circulation model. Beitr. Phys. Atmos., 57, 216-239.

Tiedtke, M. 1986: Parameterization of cumulus convection in large-scale models. Physically based modelling and simulation of climate and climatic change. Part I (Ed. M. E. Schlesinger). Published in Cooperation with NATO Scientific Affairs Division, Kluwer Academic Publishers, pp 375-425.

Tokioka, T., K. Yamazaki, A. Kitoh, and O. T. Ose, 1988: The Equatorial 30-60 day and the Arakawa-Schubert Cumulus Parameterization. Jour. Meteor. Soc., Japan, 66, 883-900.

Walker, J. and P. R. Rowntree, 1979: The effect of soil moisture on circulation and rainfall in a tropical model. Quart. Jour. R. Met. Soc., 103, 29-46.

WCP-55, 1983: World climate research report of the experts meeting on Aerosols and their climatic effects. Ed. A. Deepak and H. E. Gerber, World Climate Research Report of WMO, pp 107.

Wolfson, N., R. Atlas, Y. C. Sud, 1987: Numerical experiments related to the summer 1980 U. S. heat wave. Mon. Wea. Rev., 115, 1345-57.

Wu, M. L. , 1980: The exchange of infrared radiative energy in the troposphere. Jour. Geophys. Res., 85, 4084-4090.

Xue, Y. K., K. N. Liou, A. Kasahara, 1989: Investigation of the biogeophysical feedback on the African climate using a two dimensional model. Jour. of Climate, (in press).

Yeh, T. C., Wetherald, R. T., and Manabe, S., 1984: The effect of soil moisture on the short-term climate and hydrology change - a numerical experiment. Mon. Wea. Rev., 112, 475-490.

NASA
National Aeronautics and Space Administration

Report Documentation Page

1. Report No.	2. Government Accession No.	3. Recipient's Catalog No.
NASA TM 100771		

4. Title and Subtitle	5. Report Date
A Review of Recent Research on Improvement of Physical Parameterizations in the GLA GCM	December 1990
	6. Performing Organization Code: 911

7. Author(s)	8. Performing Organization Report No.
Y. C. Sud and G. K. Walker	91B00042
	10. Work Unit No.

9. Performing Organization Name and Address	11. Contract or Grant No.
NASA/Goddard Space Flight Center Greenbelt, MD 20771	
	13. Type of Report and Period Covered: Technical Memorandum

12. Sponsoring Agency Name and Address	14. Sponsoring Agency Code
National Aeronautics and Space Administration Washington, D.C. 20546-0001	

15. Supplementary Notes

16. Abstract

A systematic assessment of the effect of a series of improvements in physical parameterizations of the GLA GCM are summarized.

17. Key Words (Suggested by Author(s))	18. Distribution Statement
Earth-Atmosphere Interaction Studies; Precipitation Processes; Atmospheric Variability	Unclassified - Unlimited Subject Category 47

19. Security Classif. (of this report)	20. Security Classif. (of this page)	21. No. of pages	22. Price
Unclassified	Unclassified	64	